

**UNIVERSITY OF TURKISH AERONAUTICAL ASSOCIATION  
INSTITUTE OF NATURAL AND APPLIED SCIENCES**

**DEVELOPMENT OF A DUAL AXIS SOLAR CELLS TRACKING  
PROTOTYPE BASED ON A PVC FOAM MATERIAL AND AVR  
MICROCONTROLLERS**



**MASTER THESIS**

**Omar Talib KHAZRAJI**

**Electrical and Electronics Engineering Department**

**Master Thesis Program**

**NOVEMBER 2017**

**UNIVERSITY OF TURKISH AERONAUTICAL ASSOCIATION  
INSTITUTE OF NATURAL AND APPLIED SCIENCES**

**DEVELOPMENT OF A DUAL AXIS SOLAR CELLS TRACKING  
PROTOTYPE BASED ON A PVC FOAM MATERIAL AND AVR  
MICROCONTROLLERS**



**MASTER THESIS**

**Omar Talib KHAZRAJI**

**1406030036**

**Electrical and Electronics Engineering Department**

**Master Thesis Program**

**Supervisor: Asst. Prof. Dr. Hassan SHARABATY**

Omar Talib Khazraji, having student number 1406030036 and enrolled in the Master Program at the Institute of Science and Technology at the University of Turkish Aeronautical Association, after meeting all of the required conditions contained in the related regulations, has successfully accomplished, in front of the jury, the presentation of the thesis prepared with the title of: “Development of a Dual Axis Solar Cells Tracking Prototype Based on a PVC Foam Material and AVR Microcontrollers”

**Supervisor : Asst. Prof. Dr. Hassan SHARABATY**

**University of Turkish Aeronautical Association** .....

**Jury Members : Asst. Prof. Dr. Kerim Youde HAN**

**Çankaya University**



**: Asst. Prof. Dr. Özgür KELEKCI**

**University of Turkish Aeronautical Association** .....

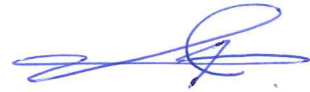
**: Asst. Prof. Dr. Hassan SHARABATY**

**University of Turkish Aeronautical Association** .....

**Thesis Defense Date: 16.11.2017**

## STATEMENT OF NON-PLAGIARISM PAGE

I hereby declare that all information in this document has been obtained and presented in accordance with academic rules and ethical conduct. I also declare that, as required by these rules and conduct, I have fully cited and referenced all material and results that are not original to this work.



30.10.2017

Omar Talib KHAZRAJI

This thesis is dedicated to:

My father, Talib Taha Khazraji

My mother, Khalida Saeed Abd Alhameed

My siblings

All my friends and lecturers who always been very supportive toward me

## **ACKNOWLEDGMENT**

First of all, praise to Allah, who has given me the beneficence in finishing this thesis. I would like to express my sincere gratitude to my advisor Dr. Hassan Sharabaty for the continuous support, and for the clear scientific guidance, precise touch and thoroughly insight discussion during the all steps of my work. Last but not least, I must express my very profound gratitude to my family; family for providing me with unfailing support and continuous encouragement through my years of study and through the process of researching and writing this thesis. This accomplishment would not have been possible without them. Thank you.

October, 2017

Omar Talib TAHA

## CONTENTS

|   |      |
|---|------|
| ACKNOWLEDGMENT .....                                  | v    |
| CONTENTS .....  | vi   |
| LIST OF FIGURES .....                                 | viii |
| LIST OF TABLES .....                                  | x    |
| LIST OF ABBREVIATIONS .....                           | xi   |
| LIST OF SYMBOLS .....                                 | xii  |
| ABSTRACT .....  | xiii |
| ÖZET .....  | xv   |
| <b>CHAPTER ONE</b> .....                              | 1    |
| <b>1. INTRODUCTION</b> .....                          | 1    |
| 1.1 Background of Study .....                         | 1    |
| 1.2 A History of Photovoltaic .....                   | 2    |
| 1.3 Literature Survey .....                           | 4    |
| 1.4 Problem Statement & Design Objectives .....       | 4    |
| 1.5 Thesis Organization .....                         | 6    |
| <b>CHAPTER TWO</b> .....                              | 7    |
| <b>2. SOLAR PANEL TRACKING SYSTEM</b> .....           | 7    |
| 2.1 Introduction .....                                | 7    |
| 2.2 Solar Tracker .....                               | 7    |
| 2.2.1 Solar Tracker Review .....                      | 7    |
| 2.2.2 Single Axis Sun Tracker .....                   | 8    |
| 2.2.3 Dual Axis Sun Tracker .....                     | 9    |
| 2.2.4 Solar Tracker Drives .....                      | 10   |
| 2.3 Modeling of Photovoltaic Module .....             | 11   |
| 2.4 Applications of Solar Energy .....                | 15   |
| 2.5 Advantages of The Solar Energy .....              | 18   |
| 2.6 Obstacles of Spreading The Solar Energy .....     | 18   |
| <b>CHAPTER THREE</b> .....                            | 19   |
| <b>3. METHODOLOGY AND PROPOSED PROTOTYPE</b> .....    | 19   |
| 3.1 Introduction .....                                | 19   |
| 3.2 Drawing of The Mechanical Parts .....             | 19   |
| 3.3 Installation of The Mechanical Parts .....        | 22   |
| 3.4 Block Diagram .....                               | 25   |
| 3.5 Components of The Proposed Prototype .....        | 26   |
| 3.5.1 The Microcontroller Unit .....                  | 26   |
| 3.5.2 The Rotation Unit .....                         | 27   |
| 3.5.3 The Sensing Unit .....                          | 29   |
| 3.5.4 Other Components .....                          | 30   |
| 3.6 Solar Cells Connections .....                     | 32   |
| 3.7 Inputs and Outputs to The Arduino Uno Board ..... | 33   |
| 3.8 Simulation of The Proposed System .....           | 33   |

|  |           |
|--|-----------|
| 3.9 Working Principle of The Proposed System.....                                | 34        |
| 3.10 The LDRs Resistance With Different Angles of The Sun.....                   | 36        |
| 3.11 Calculation of The Fixed Series Resistance.....                             | 37        |
| 3.12 Flowchart of The Tracking Operation .....                                   | 38        |
| 3.13 Our Final Prototype.....  | 39        |
| <b>CHAPTER FOUR.....</b>   | <b>40</b> |
| <b>4. RESULTS AND DISCUSSION .....</b>   | <b>40</b> |
| 4.1 The Weight of Our Proposed Design.....                                       | 40        |
| 4.2 Results of Different Cells Connection Cases.....                             | 41        |
| 4.2.1 Parallel Solar Cells Connection.....                                       | 41        |
| 4.2.2 Series Solar Cells Connection .....  | 42        |
| 4.2.2.1 Switching DC relay using an interval of 5 minutes<br>for 12 hours .....  | 43        |
| 4.2.2.2 Switching DC relay using an interval of 10 minutes<br>for 12 hours ..... | 44        |
| 4.2.2.3 Switching DC relay using an interval of 20 minutes<br>for 12 hours ..... | 45        |
| 4.2.2.4 Switching DC relay using an interval of 30 minutes<br>for 12 hours ..... | 46        |
| 4.2.2.5 Switching DC relay using an interval of 40 minutes<br>for 12 hours ..... | 47        |
| 4.2.2.6 Switching DC relay using an interval of 50 minutes<br>for 12 hours ..... | 48        |
| 4.2.2.7 Switching DC relay using an interval of 55 minutes<br>for 12 hours ..... | 49        |
| 4.2.2.8 Switching DC relay using an interval of 1 hour for<br>12 hours.....      | 50        |
| 4.2.2.9 Switching DC relay using an interval of 2 hours for<br>12 hours.....     | 51        |
| 4.2.2.10 Switching DC relay using an interval of 3 hours for<br>12 hours.....    | 52        |
| 4.2.2.11 Switching DC relay using an interval of 4 hours for<br>12 hours.....    | 53        |
| 4.2.2.12 Switching DC relay using an interval of 6 hours for<br>12 hours.....    | 54        |
| 4.3 Energy Consumption of The Prototype .....                                    | 55        |
| 4.4 The Generated Energy Gain.....   | 57        |
| 4.5 Efficiency of The Proposed Prototype .....                                   | 58        |
| <b>CHAPTER FIVE.....</b>   | <b>60</b> |
| <b>5. CONCLUSIONS AND FUTURE WORKS.....</b>                                      | <b>60</b> |
| 5.1 Conclusions.....   | 60        |
| 5.2 Future Works .....   | 60        |
| <b>REFERENCES.....</b>   | <b>62</b> |
| <b>CURRICULUM VITAE.....</b>   | <b>64</b> |



## LIST OF FIGURES

|                    |  |    |
|--------------------|--|----|
| <b>Figure 2.1</b>  | : Single axis solar tracker.....   | 9  |
| <b>Figure 2.2</b>  | : Dual axis solar tracker .....  | 10 |
| <b>Figure 2.3</b>  | : The passive tracker .....  | 10 |
| <b>Figure 2.4</b>  | : The active tracker .....   | 11 |
| <b>Figure 2.5</b>  | : Ideal PV cell with single-diode .....                                      | 11 |
| <b>Figure 2.6</b>  | : PV circuit model with single-diode and series resistance .....             | 12 |
| <b>Figure 2.7</b>  | : PV circuit model with a single-diode, series and parallel resistances..... | 13 |
| <b>Figure 2.8</b>  | : PV circuit model with two-diode, series and parallel resistances.....      | 14 |
| <b>Figure 2.9</b>  | : The I-V characteristic curve of a solar panel.....                         | 15 |
| <b>Figure 2.10</b> | : Photovoltaic panels in power plant.....                                    | 16 |
| <b>Figure 2.11</b> | : Photovoltaic panels in homes .....   | 16 |
| <b>Figure 2.12</b> | : Photovoltaic panels for commercial usage .....                             | 17 |
| <b>Figure 2.13</b> | : The solar lighting.....  | 17 |
| <b>Figure 3.1</b>  | : Parts of the upper section.....  | 20 |
| <b>Figure 3.2</b>  | : Parts of the middle section .....  | 20 |
| <b>Figure 3.3</b>  | : Parts of the lower section.....  | 21 |
| <b>Figure 3.4</b>  | : The base of the design .....   | 21 |
| <b>Figure 3.5</b>  | : Connection of the lower section .....                                      | 22 |
| <b>Figure 3.6</b>  | : Connection of the middle section .....                                     | 23 |
| <b>Figure 3.7</b>  | : Connection of the upper section .....                                      | 24 |
| <b>Figure 3.8</b>  | : The final proposed prototype (mechanical portion) .....                    | 25 |
| <b>Figure 3.9</b>  | : Block diagram of the proposed Prototype .....                              | 26 |
| <b>Figure 3.10</b> | : The simulation and working of the arduino uno board .....                  | 27 |
| <b>Figure 3.11</b> | : The simulation and parts of the servo motors .....                         | 28 |
| <b>Figure 3.12</b> | : Vertical and horizontal servo motors practically.....                      | 28 |
| <b>Figure 3.13</b> | : Servo motors connections to the Arduino board .....                        | 29 |
| <b>Figure 3.14</b> | : The simulation and position of the four LDRs .....                         | 29 |
| <b>Figure 3.15</b> | : The fixed resistances (360 $\Omega$ ) practically.....                     | 30 |
| <b>Figure 3.16</b> | : Voltage regulation LM2596 .....  | 30 |
| <b>Figure 3.17</b> | : The thermometer.....   | 31 |
| <b>Figure 3.18</b> | : Load (10 W 300 $\Omega$ ) with the measuring voltage and current .....     | 31 |
| <b>Figure 3.19</b> | : 10 solar cells .....   | 32 |
| <b>Figure 3.20</b> | : Series solar cells connection.....   | 32 |
| <b>Figure 3.21</b> | : Parallel solar cells connection .....                                      | 33 |
| <b>Figure 3.22</b> | : The completed simulation of the proposed tracking system .....             | 34 |
| <b>Figure 3.23</b> | : Measuring the LDR resistance .....   | 36 |
| <b>Figure 3.24</b> | : Cases of measuring the fixed series resistance.....                        | 38 |
| <b>Figure 3.25</b> | : Flowchart of the tracking operation .....                                  | 39 |
| <b>Figure 3.26</b> | : The proposed prototype.....  | 39 |

|                    |   |    |
|--------------------|---|----|
| <b>Figure 4.1</b>  | : The reference prototype and our proposed prototype.....           | 41 |
| <b>Figure 4.2</b>  | : Interpretation data of power of solar panel 0.12 W .....          | 42 |
| <b>Figure 4.3</b>  | : Rotating vs. static system for switching interval of 5 mins.....  | 43 |
| <b>Figure 4.4</b>  | : Rotating vs. static system for switching interval of 10 mins..... | 44 |
| <b>Figure 4.5</b>  | : Rotating vs. static system for switching interval of 20 mins..... | 45 |
| <b>Figure 4.6</b>  | : Rotating vs. static system for switching interval of 30 mins..... | 46 |
| <b>Figure 4.7</b>  | : Rotating vs. static system for switching interval of 40 mins..... | 47 |
| <b>Figure 4.8</b>  | : Rotating vs. static system for switching interval of 50 mins..... | 48 |
| <b>Figure 4.9</b>  | : Rotating vs. static system for switching interval of 55 mins..... | 49 |
| <b>Figure 4.10</b> | : Rotating vs. static system for switching interval of 1 hrs.....   | 50 |
| <b>Figure 4.11</b> | : Rotating vs. static system for switching interval of 2 hrs .....  | 51 |
| <b>Figure 4.12</b> | : Rotating vs. static system for switching interval of 3 hrs .....  | 52 |
| <b>Figure 4.13</b> | : Rotating vs. static system for switching interval of 4 hrs .....  | 53 |
| <b>Figure 4.14</b> | : Rotating vs. static system for switching interval of 6 hrs .....  | 54 |
| <b>Figure 4.15</b> | : Energy consumption curve.....                                     | 56 |
| <b>Figure 4.16</b> | : Generated energy gain curve.....                                  | 58 |
| <b>Figure 4.17</b> | : Efficiency curve of the proposed prototype .....                  | 59 |
| <b>Figure 5.1</b>  | : STM32 Nucleo-64 development board with STM32F401RE<br>MCU .....   | 61 |

## LIST OF TABLES

|  |    |
|--|----|
| <b>Table 3.1</b> : The value of LDR resistance .....   | 36 |
| <b>Table 4.1</b> : Comparison with reference prototype.....  | 41 |
| <b>Table 4.2</b> : Energy consumption of the prototype for different intervals of<br>time .....    | 56 |
| <b>Table 4.3</b> : Generated energy gain of the prototype for different intervals of<br>time ..... | 57 |
| <b>Table 4.4</b> : Efficiency percentage of the proposed prototype .....                           | 58 |



## LIST OF ABBREIVIATIONS

|             |  |
|-------------|--|
| <b>PV</b>   | : Photo-Voltaic                            |
| <b>HIT</b>  | : Heterojunction with Intrinsic Thin Layer |
| <b>PC</b>   | : Personal Computer                        |
| <b>DC</b>   | : Direct Current                           |
| <b>AC</b>   | : Alternating Current                      |
| <b>PWM</b>  | : Pulse Width Modulation                   |
| <b>LDR</b>  | : Light Dependent Resistor                 |
| <b>DAQ</b>  | : Data Acquisition                         |
| <b>PVC</b>  | : Polyvinyl Chloride                       |
| <b>USB</b>  | : Universal Serial Bus                     |
| <b>CNC</b>  | : Computer Numerical Control               |
| <b>PLC</b>  | : Programmable Logic Controller            |
| <b>GA</b>   | : Genetic Algorithm                        |
| <b>PSO</b>  | : Particle Swarm Optimization              |
| <b>FPGA</b> | : Field Programmable Gate Array            |
| <b>ANN</b>  | : Artificial Neural Network                |
| <b>FLC</b>  | : Fuzzy Logic Controller                   |
| <b>LCD</b>  | : Liquid Crystal Display                   |
| <b>GSM</b>  | : Global System for Mobile Communication   |
| <b>MHz</b>  | : Mega Hertz                               |

## LIST OF SYMBOLS

|            |              |
|------------|--------------|
| <b>%</b>   | : Percentage |
| <b>n°C</b> | : Celsius    |
| <b>n°</b>  | : Degree     |
| <b>W</b>   | : Watt       |
| <b>A</b>   | : Ampere     |
| <b>V</b>   | : Volt       |
| <b>Ω</b>   | : Ohm        |
| <b>J</b>   | : Joule      |
| <b>K</b>   | : Kilo       |
| <b>M</b>   | : Mica       |

## **ABSTRACT**

### **DEVELOPMENT OF A DUAL AXIS SOLAR CELLS TRACKING PROTOTYPE BASED ON A PVC FOAM MATERIAL AND AVR MICROCONTROLLERS**

KHAZRAJI, Omar Talib

Master Thesis, Department of Electrical and Electronics Engineering

Thesis Supervisor: Asst. Prof. Dr. Hassan SHARABATY

November 2017, 64 pages

With a view to evolve additional solar energy and to raise the efficiency of the solar photovoltaic panels, tracking systems are used to follow the sun position and to let the solar photovoltaic panels head for the sun as long as possible.

In this thesis, we propose to use PVC foam material instead of the other materials such as Iron and plastic in order to develop a dual axis solar panel tracking prototype based on AVR microcontrollers. Compared to other materials, PVC foam withstands more temperatures and can reduce the design weight and power consumption. In addition, this work proposes to discretize the tracking operation of sun position by using a switching DC relay, and to study the effect of the consumed energy, by the control circuit and the motors, on the total generated energy of the system, and then to determine the optimal DC relay timing period. Finally, we discuss the advantages of connecting solar cells in series regarding the solar panel output voltage.

The mechanical parts of our system were drawn by using AutoCAD 2017 and accomplished with aid of the foam cutting machine CNC (Computer Numerical Control). The simulation design and the control circuit of our prototype developed by using PROTEUS 8, and the practical implementation of the tracking prototype were controlled by AVR microcontroller.

The experimental work shows that compared to the static solar system, our proposed dual axis solar tracking prototype is more effective for absorbing the highest sunlight source with increasing of the average power by 34%. Moreover, our measurements proved that the optimal interval for discrete tracking system is 20 minutes that gives the maximum achieved efficiency of our prototype, i.e. 34%. Compared to the continuous tracking system, the optimal tracking interval saves 89.45% of the consumed energy by the control circuit.

**Key words:** Dual axis solar trackers, Discrete sun tracking, Solar cells, AVR microcontrollers, PVC foam material.



## ÖZET

# PVC KÖPÜK MATERYAL VE AVR MİKRO KONTROLÖRLERE DAYALI ÇİFT EKSENLİ SOLAR HÜCRE TAKİP PROTOTİPİNİN GELİŞTİRİLMESİ

KHAZRAJI, Omar Talib

Yüksek Lisans Tezi, Elektrik ve Elektronik Mühendisliği Bölümü

Tez Danışmanı: Yrd. Doç. Dr. Hassan SHARABATY

Kasım 2017, 64 sayfa

Ek solar enerjilerin geliştirilmesi ve solar fotovoltaik panellerin verimliliğinin artırılması ışığında, güneşin konumunun belirlenmesi ve mümkün olduğu kadar uzun süreyle solar fotovoltaik panellerin güneşe bakmasını sağlamak için takip sistemleri kullanılmaktadır.

Bu tezde, AVR mikro kontrolörlere dayalı çift eksenli solar panel takip prototipi geliştirmek amacıyla demir ve plastik gibi diğer materyallerin yerine PVC köpük materyali kullanmayı önermekteyiz. Diğer materyaller ile karşılaştırıldığında, PVC köpük materyali, daha yüksek sıcaklıklara dayanmaktadır ayrıca tasarım ağırlını ve güç tüketimini azaltabilmektedir. İlaveten, bu çalışma, anahtarlı DA röle kullanarak güneşin konumunu takip işlemini kesintili hale getirmeyi ayrıca kontrol devresi ve motorların tükettiği enerjinin sistemin toplam ürettiği enerjisi üzerindeki etkisini incelemeyi ve daha sonra optimum DA röle zamanlama sürelerini tespit etmeyi amaçlamaktadır. Son olarak, solar panel çıkış voltajına ilişkin solar hücreleri seri olarak bağlamanın avantajlarını tartışmaktayız.

Sistemimizin mekanik parçaları, AutoCAD 2017 programı kullanarak çizilmiş ve köpük kesme makinesi CNC (Bilgisayarlı Sayısal Denetim) yardımı ile tamamlanmıştır. Simülasyon tasarımı ve PROTEUS 8 kullanılarak geliştirilen prototipimizin kontrol devresi ve takip prototipinin pratikte uygulamaya koyulması AVR mikro kontrolör tarafından denetlenmektedir.



Deneyisel çalışma, statik solar sisteme kıyasla, önerdiğimiz çift eksenli solar takip prototipinin, ortalama gücü %34 arttırarak güneş ışığı kaynağını en yüksek şekilde absorbe etme konusunda daha verimli olduğunu göstermektedir. İlaveten, ölçümlerimiz, kesintili takip sistemi için optimum aralığın, prototipimizde elde edilen %34 maksimum verimliliği sağlayan 20 dakika olduğunu ortaya koymuştur. Sürekli takip sistemiyle karşılaştırıldığında, optimum takip aralığı, kontrol devresi tarafından tüketilen enerjide %89.45 tasarruf etmektedir.

**Anahtar kelimeler:** Çift eksenli solar takipçiler, kesintili güneş takibi, Solar hücreler, AVR mikro kontrolörleri, PVC köpük materyali.



## **CHAPTER ONE**

### **INTRODUCTION**

#### **1.1 Background of Study**

At the present time, the use of fossil fuel energy such as coal, natural gas, and nuclear energy etc. has always been contributing significantly in regard of the utilization and the development of industrial society. The generation of electric power by using sources of renewable energy has begun undertaking a dominant role in fulfilling the demands of electrical energy. The detraction of fossil fuel resources is anticipated to diminish within the next hundred years [1].

The renewable energy is the one that is generated by the natural surroundings which are replenished continuously. The energy sources such as the wind, sunlight, geothermal heat, water, and biomass are renewed constantly. Solar energy is the most effective and efficient energy to produce electricity throughout the use of the renewable energy. Specially, in countries where the warm climate is mostly dominant and solar energy is looked upon as one of the predominate sources of energy [2].

The solar energy is considered as the fastest growing among the other renewable energy technology, since due to the primary source; it is costless on continual bases, accessible, plentiful, nonpolluting and clean. The solar radiation is counted according to the quantity of solar energy which falls on solar PV panel after a period of time, called the solar irradiation. The Solar radiation is formed of three combinations; direct, diffused and reflected radiations. The solar energy decreases when the weather is cloudy and wet, thus the solar PV panel is unable to receive sufficient sun radiation to produce electricity [2].

Also, there is another problem is that when the solar photovoltaic (PV) has low efficiency in producing maximum output power which is derived from sunlight. To

fix this problem up, several works have been examined to increase the efficiency of the output power by using the solar tracking system. The solar tracking system is used to maintain the solar PV panels perpendicular to sun radiation. The system is also regarded as a Mechatronic system of merged elements of mechanics, electronics and technology of information [3]. Bases on annual estimation, up to 35% are to increase the efficiency of production of energy which was accommodated by solar tracking system [4].

## **1.2 A History of Photovoltaic**

The physical phenomenon that converts the sunlight to electricity-the photo voltaic (or PV) effect-was firstly discovered in 1839 by the French physicist Edmund Becquerel. He observed that a voltage appeared when one or two similar electrodes in a weak conducting solution were illuminated. The photovoltaic effect was firstly studied in solids, especially in selenium in the 1870s by Adams and Day. In 1880s, the selenium photovoltaic cells exhibited an efficiency rate from 1% to 2% in regard of converting light into electricity. Since the selenium responds to light in the visible spectrum manners, it was vastly used by the emerging field of photography for photo metric (light-measuring) devices, and it is yet utilized for that purpose today. Selenium cells are considered impractical as converters of energy; although, due to their high cost when compared to the amount of power they produce. In the 1920s and 1930s, each of Lange, Grondahl and Schottky made a pioneering work on selenium and cuprous oxide photovoltaic cells. Developments in quantum mechanics built the theoretical foundation for our present concept of photovoltaic. Scientists achieved a big advancement during 1940s and 1950s in regard of solar cell technology through developing a way to grow single crystals of silicon, called the Czochralski (CZ) method. Early in 1941, Bell Laboratories had fashioned a photovoltaic device which is made from single CZ crystal material. However, silicon solar cells didn't become practical until 12 years later when scientists had developed a method of diffusing certain desirable impurities of the silicon. Simultaneously, researchers made a major advancement in regard of cadmium sulfide, cadmium telluride and gallium arsenide of solar cells. By 1954, many studies at Bell laboratories and at RCA documented solar cells of efficiencies conversion up to 6%. As with advanced fabrication processes, our understanding of solar-cell operations

has also grown. In turn, this led to a better designing and even higher cell efficiencies. Hoffman Electronics Corporation produced a terrestrial PV cell with the efficiency of energy conversion of nearly 14% by 1958. During the same period, Bell Telephone Company had tested a PV array of rural telephone transmission near Americus, Georgia. The solar cell performance was good; however, there were found to cost more compared with conventional battery or other utility power alternatives. Even though PV cells weren't considered cost-effective for terrestrial applications, but a practical use was found in the new U.S. space program. During 1958, Vanguard Space Satellite carried an array of photovoltaic to power its radio. The successful performance of these solar cells had made outer space PV's primary object. Developments concerning solar cell technology which followed mainly depended on PV being used in other space programs to research in regard of solid-state transistor industry, which makes the use of similar materials and physical mechanisms very familiar. In spite of that, concerning the 'energy crises' in 1970s, the interest was replenished in regard of photovoltaic for terrestrial applications. In turn, this stimulated research is to improve the existing solar cell technologies and to develop a new solar cell materials and designs [5].

Barnett developed the polycrystalline silicon thin film cell by 1980s; on the other hand, Martin Green had replaced the silicon serigraphy with a silicon solar cell of greater surface area in order to catch the sun rays with a tiny laser-etched grooves where the wires (contacts) which are carrying the electric current are buried and can led to a 20% more efficient cells.

The first modules which used triple junction amorphous silicon cells were first commercialized by Sharp in 1997, in addition; Sanyo achieved a 22% efficiency of research level with its HIT solar cells by 2007. The HIT (heterojunction with intrinsic thin layer) solar cell is composed of a single thin crystalline silicon wafer which is surrounded by an ultra-thin amorphous silicon layers. HIT cell structure enables and allows an improvement in regard of overall output by reducing the combination loss through surrounding the layers of energy generation of single thin crystalline silicon with higher quality ultra-thin layers of amorphous silicon. On the other hand, a highly efficient GaAs cells were also developed in order to power spacecraft that now exploiting the recent discovery of the nearly perfected growth of GaAs crystals in addition to quantum-well solar cells which are based on the same

material and they are most likely to facilitate a new way to a third kind of solar cells generation [6].

### **1.3 Literature Survey**

The first proposed solar tracking systems were single axis tracker as in the one introduced by T. Tudorache and L. Kreindler [7] to ensure the optimization of the conversion of the solar energy into electricity by properly orienting the PV panel in accordance with the real position of the sun. In 2011, S. Ozcelik, H. Prakash, R. Chaloo [8] simulated and implemented the most efficient algorithm to control the dual-axes solar tracker which could rotate in direction of azimuth and elevation. The simulation provided the angels of the tracker which position the solar panel along the sun rays with maximum solar irradiation that is absorbed by the panel. Later on, Alberto Dolara, Francesco Grimaccia, Sonia Leva, Marco Mussetta, Roberto Faranda, & Moris Gualdoni [9] had conducted an analysis of performance of photovoltaic (PV) tracking system. In order to study the efficiency which was based on the results of the experiment of specific power plant, and to analyze a single-axis system by taking into consideration the different indexes of better characterization of overall system performance. The data of the experiment had been collected by an on-site monitoring system over the period of one year, concluding final considerations and comparison results of PV system efficiency.

In 2013, Ali Reyadh Waheed [10] proposed simulation design based on a single axis solar photovoltaic panel tracker which was capable to track the sun throughout the year. Kinematics of the mechanical part of the tracking system was simple and can easily be controlled by the microcontroller using the digital data (which is originally the difference voltage between the two sensors) from the ADC. Two sides of free rotation (East and West) were feasible. The 89C51 microcontroller was used to control the position of DC motors which ensured point to point intermittent motion resulting from the DC motor. As a result of the high-resolution tracking system, the percentage power obtained from the solar panel was increased by 34.533%. After that, Ahmad Amsyar Bin Azman [11] designed and implemented a dual axis tracker prototype using an Arduino Uno microcontroller. The prototype followed the sun position by using combination of servo and DC motors to increase the overall efficiency by 8-10% compared to the static system. In 2015, Muhammad

Amirul Asyraf Bin Shukor [12] built a solar tracker prototype to track the sun position by using economic components. He tested the prototype for seven days and determined the variance value. Finally, he noted that the variance value for one week efficiency was small by 7.715% and it was so close to the average value.

In 2016, Vijayalakshmi K [13] introduced a control system which will lead to a better photovoltaic (PV) alignment of arrays in accordance with sunlight and also to gain the solar power. The system changed the direction in two different axes in order to trace the coordinates of sunlight by detecting the differences between the position of the sun and the panel. A hardware testing concerning the proposed system was conducted to check the system ability in tracking and following the sunlight in efficient manners.

The previous studies show that two types of solar panel tracking prototypes were proposed:

- The first one contains big solar panels and can be used for energy generating purposes because the total average of the generated energy is higher than the total energy of the consumption.
- The second type was dedicated for research purposes in labs and universities and was contains small solar panels. The main problem here is that the total energy of the consumption of these small prototypes is higher than the total average of the generated energy.

#### **1.4 Problem Statement & Design Objectives**

As we mentioned in the previous section that the old dual axis solar panel laboratory prototypes, the consumed energy by the control circuit and the motors is higher than the total output of the generated energy by the solar panels. Furthermore, those systems were heavy that increase the power consumption.

In this thesis, we propose to use the PVC foam material instead of the previous materials in order to withstand high temperatures and to reduce the design weight and power consumption. Also, we propose to use a switching DC relay in order to discretize the tracking operation, to study the effect of the consumed energy through the control circuit and motors on the total average of the generated energy by the system, and then to determine the optimal DC relay switching interval.

## **1.5 Thesis Organization**

This dissertation is divided into five chapters. We start in Chapter 1 by giving the background information, summarizing the literature review of the research subject, problem statement, work objectives and thesis organization. Then in Chapter 2, we talk about the solar tracking system technologies, modeling of photovoltaic module, applications of solar energy, advantages of the solar energy and obstacles of spreading the solar energy. Then, in Chapter 3, we display the designing and implementing of the proposed dual axis solar cells tracking prototype. In Chapter 4, we test the proposed dual axis solar cells tracking prototype. Finally, in Chapter 5, we show the Conclusions from research and suggestions for future works.

## **CHAPTER TWO**

### **SOLAR PANEL TRACKING SYSTEM**

#### **2.1 Introduction**

The necessity of the tracking system for solar PV panel arises to extract the maximum amount of solar energy. The work which is announced in this thesis comprises the design of the control system of the dual axis solar cells tracking system for the solar PV panel. The tracking system can be installed in the areas where solar energy is rich such as roofs, open areas, deserts, etc.

The dual axis solar PV panel has the ability to move in two directions (vertical and horizontal directions). The vertical and the horizontal motions of the proposed system obtained by taking the difference voltage between four LDRs oriented on both sides of the X-axis and Y-axis. The microcontroller (Arduino Uno board) has been used to control the rotation of the servo motors.

This tracking system makes the solar PV array more efficient by keeping the panel's face perpendicular to the sun and therefore, it can extract maximum amount of solar energy which leads to increase the overall efficiency.

The discussion in this chapter focuses on the solar tracking system technologies, modeling of photovoltaic module, applications of solar energy, advantages of the solar energy and obstacles of spreading the solar energy.

#### **2.2 Solar Tracker**

##### **2.2.1 Solar Tracker Review**

The solar tracker is a device that directs a payload toward the sun. The utilization of the solar trackers can raise electricity production about one-third, and



some claim up to 40% in some areas, compared to the fixed angle modules. In any solar energy application, the transformation efficiency is improved when the modules are continually adjusted to the optimum angle as the sun perforates the sky. As improved efficiency means improved performance, the utilization of the trackers can totally make a difference to the income from large plant.

Commercial purpose of solar tracking system:

1. Increased production of solar panel.
2. Maximum panel efficiency.
3. Maximize power per unit area.
4. Capable of extracting energy during the day [14].

A Sun-tracking mechanism raises the solar energy amount that can be received by the solar collectors or photo-voltaic modules. Consequently, this would lead to an increase in the production of daily and annual output power harnessed. The utilization of the tracking system is more expensive and more complicated than the fixed system assemblies. However, it can become profitable in many cases because they provide more output power throughout the year and in many cases this increase exceeds 25% [15].

The solar power generation works best when it is situated directly towards the sun, so the solar tracker can raise the efficiency of such equipment in any fixed position. The solar panels must be perpendicular to the sun radiation to generate maximum power. Deviating from this optimum angle will reduce the energy generation efficiency from the panels [16]. The solar system efficiency depends on the degree of use and transformation of the sun's rays. By applying the energy balance on the solar panel, the reference is done to the surface that absorbs the incoming radiation and to the balance between the energy inflow and the energy outflow [16]. The position of the sun in the sky varies with each seasons (height) and day time as the sun moves through the sky. Consequently, there are also two kinds of solar tracker, "Single axis sun tracker" and "Dual axis sun tracker".

### **2.2.2 Single Axis Sun Tracker**

In this kind of systems, it is possible to move the panels on a single path which is usually an east-west direction. During the day, the sun rises from east and sets in the west. In such systems, the panel moves according to the movement of the sun and

attempts to stay perpendicular to the angle of the sun radiation. But the sun also moves in a north-south path as shown in Figure (2.1) [17]. In addition, the single axis solar trackers can be any of the horizontal or the vertical axes. The use of the horizontal kind is concentrated in tropical areas where the sun gets very high at noon, but the day is short. The use of the vertical kind in high latitudes (as is the case in UK) is concentrated where the sun does not get too high, but the summer days can be very long [14].

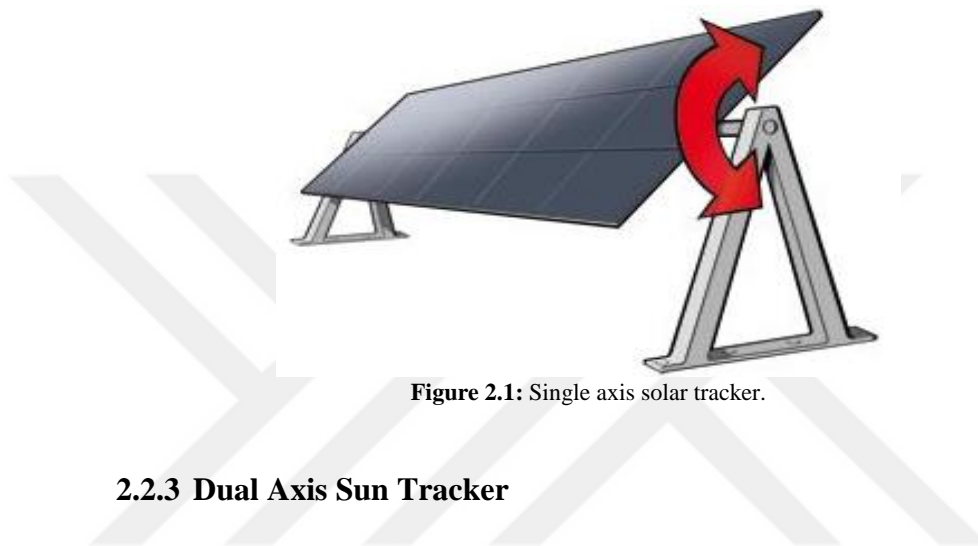


**Figure 2.1:** Single axis solar tracker.

### **2.2.3 Dual Axis Sun Tracker**

The panels are capable of moving along both east-west and north-south directions in such systems; hence, they are usually perpendicular to the sun ray's direction and receive the highest amount of the sunray. Determining the angle of panels at every moment has two methods. In some trackers, a pair of optical sensors causes an imbalance guiding of controller to rotate in a direction which makes the imbalance zero if the panel is not perpendicular to the sun radiation. In some other panels, the shining angle of the sun in each time during the year is determined by utilizing the planetary relations and the parameters which feed these information to the microcontroller, the tracker will position the panel in the desired angle [17]. The double axes solar tracker consists of both horizontal and vertical axes and can track the sun's motion anywhere in the world with extreme precision. Such system is used in controlling astronomical telescopes, and much software is available in order to automatically predict and track the sun motion in the sky. The dual axis trackers can track the sun both E-W and N-S to add more power output (approx. 40% gain) and convenience as shown in Figure (2.2) [14].

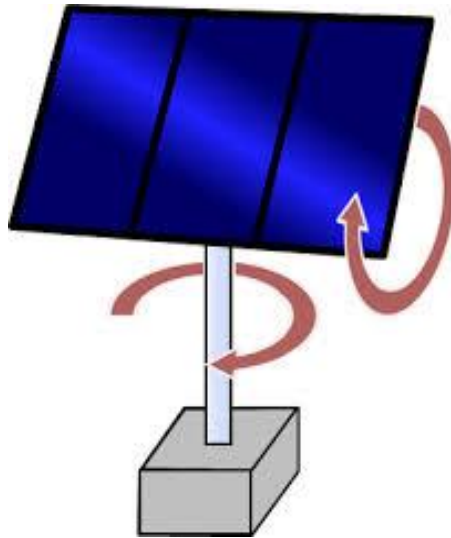


**Figure 2.2:** Dual axis solar tracker.

#### **2.2.4 Solar Tracker Drives**

The drives of solar tracker are divided into three main kinds depending on the drive type and sensing or positioning of the system which incorporate, “Passive Trackers”, “Active Trackers”, and “Open Loop Trackers”.

The passive tracker shown in Figure (2.3) is utilized a compressed gas fluid in two canisters on each place of the W-E tracker. The mechanism is in such a way that if one side cylinder is heated and the other side of piston raises, it will cause the panel to tilt over the sunny side. This can affect the tracker balance and caused it to tilt. This system is considered very reliable and requires less maintenance [14].



**Figure 2.3:** The passive tracker.

However, the active trackers shown in Figure (2.4) measure the intensity of light from the sun by using photo sensors to locate where the solar modules should be forming. The light sensors are formed on the tracker at different zones in particularly shaped holders. If the sun is not facing the tracker directly, there will be a difference in intensity of light on one photo sensor compared to another and this give rises to locate in which direction the tracker has to rotate with the assist of the DC motor or the stepper so as to be facing the sun [14].



Figure 2.4: The active tracker.

Whereas, “Open Loop Trackers” have no sensors but instead determine the sun position by pre-recorded data for a particular site [14].

### 2.3 Modeling of Photovoltaic Module

To develop an equivalent circuit for a PV cell, it is important to understand the physical configuration of the components of the cell as well as the electrical properties of each element. The ideal equivalent circuit of a PV cell is a single diode in parallel with a current source [18].

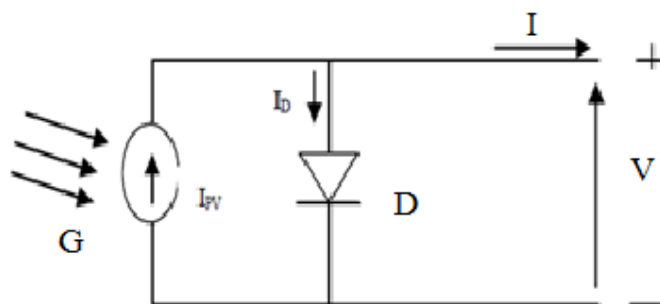


Figure 2.5: Ideal PV cell with single-diode [18].

The equation for the output current is given by:

$$I = I_{PV} - I_D \quad (2.1)$$

Where

$$I_D = I_0 \left[ \exp\left(\frac{V}{AV_T}\right) - 1 \right] \quad (2.2)$$

Then equation (2.1) becomes:

$$I = I_{PV} - I_0 \left[ \exp\left(\frac{V}{AV_T}\right) - 1 \right] \quad (2.3)$$

$I_0$  is the diode saturation current.

$V_T = \frac{N_s * k * T}{q}$  is the thermal voltage of a PV module.

$N_s$  cells connected in series.

$q$  is the electron charge value ( $>0$ ) ( $1.602 * 10^{-19}$  coulombs).

$K$  is the Boltzmann constant ( $1.38 * 10^{-19}$  J/K).

$T$  is the absolute temperature in Kelvin.

$A$  is the diode ideality factor.

More accuracy and complexity can be introduced to the previous model by adding a series resistance  $R_s$ . The circuit diagram of this model is shown in Figure (2.6).

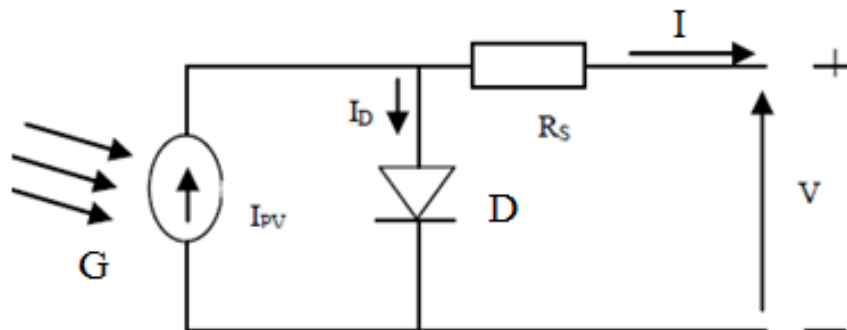


Figure 2.6: PV circuit model with single-diode and series resistance [18].

For the same temperature and irradiation conditions, the series resistance inclusion in the model implies the utilization of a recurrent equation to calculate the output current in the terminal voltage function. The I-V characteristics of the solar cell are given by:

$$I = I_{PV} - I_0 \left[ \exp \left( \frac{V + I R_S}{A V_T} \right) - 1 \right] \quad (2.4)$$

The PV model devices are essentially explained in two different models with series and parallel resistances: Single-diode model with series and parallel resistances and double diode model with series and parallel resistances.

The photovoltaic cell models have been for a long as a source for the description of the photovoltaic cell behavior. The most common model is used to predict energy production in the photovoltaic cell modeling by applying the single diode lumped circuit model. In the single diode model, there is a current source parallel to a diode. The current source represents light-generated current  $I_{pv}$  that varies linearly with solar irradiation. This is the simplest and the most widely used model as it offers a good compromise between simplicity and accuracy [18].

Figure (2.7) shows the single diode equivalent circuit model of PV cell which is commonly used in many studies and provides sufficient accuracy for most applications.

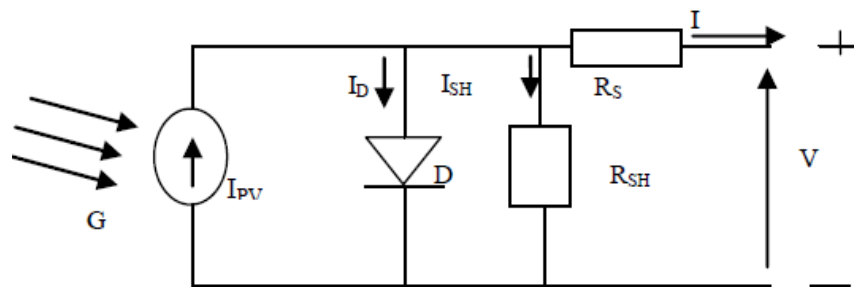


Figure 2.7: PV circuit model with a single-diode, series and parallel resistances [18].

A more practical model can be seen in Figure (2.7), where  $R_S$  represents the equivalent series resistance and  $R_{SH}$  the parallel resistance. According to and based on the equivalent circuit of a photovoltaic panel, its characteristic equation is deduced.

$$I = I_{PV} - I_0 \left[ \exp \left( \frac{V+I \cdot R_S}{A \cdot V_T} \right) - 1 \right] - \left( \frac{V+I \cdot R_S}{R_{SH}} \right) \quad (2.5)$$

This model yields more accurate result than the PV model with series resistances  $R_S$  but at the expense of longer computational time [18].

In the model below, an extra diode is attached in parallel to the circuit of single-diode model as seen in Figure 2.7. This diode is included to provide a more accurate I-V characteristic curve that considers for the difference in flow of circuit at low current values due to the charge combination in the semiconductor's depletion [18].

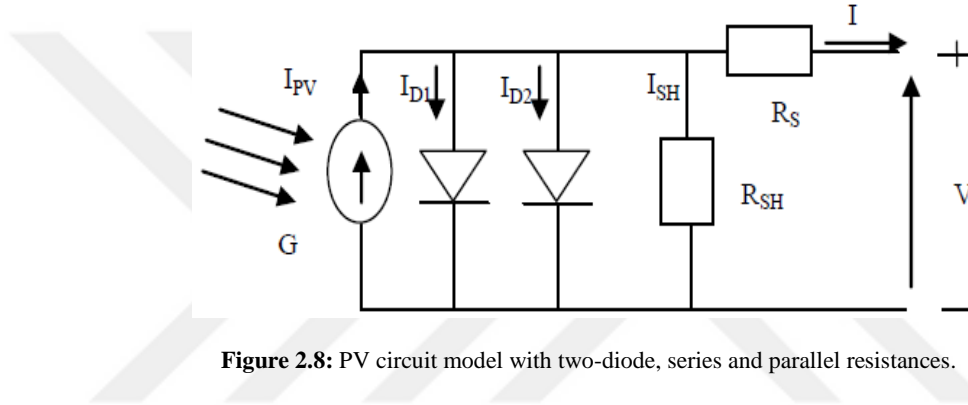


Figure 2.8: PV circuit model with two-diode, series and parallel resistances.

The accuracy of these models is more than the single diode model but there are some difficulties to resolve the equation. For simplicity, the single diode model of Figure (2.7) is selected and is utilized in this work. The basic equation (2.4) of two-diode model of the PV cell is given by the following equation:

$$I = I_{PV} - I_{D1} - I_{D2} \quad (2.6)$$

Where

$$I_{D1} = I_{01} * \left[ \exp \left( \frac{V}{A_1 * V_T} \right) - 1 \right] \quad (2.7)$$

$$I_{D2} = I_{02} * \left[ \exp \left( \frac{V}{A_2 * V_T} \right) - 1 \right] \quad (2.8)$$

After the combination of equations (2.7) and (2.8) and the inclusion of additional parameters  $R_S$  and  $R_{SH}$ , the equation (2.6) becomes:

$$I = I_{PV} - I_0 * \left[ \exp\left(\frac{V+R_s*I}{A_1*V_T}\right) - 1 \right] - I_{02} * \left[ \exp\left(\frac{V+R_s*I}{A_2*V_T}\right) - 1 \right] - \left(\frac{V+R_s*I}{R_{SH}}\right) \quad (2.9)$$

Where

$I_{01}$  is the reverse saturation current due to diffusion.

$I_{02}$  is the reverse saturation current due to recombination in the space charge layer.

$A_1=1$  is the diode D1 ideality factor and  $A_2 \geq 1.2$  is the diode D2 ideality factor. All others parameters are explained previously [18].

“From equation (2.5) one can find the I-V characteristic curve of a solar panel”, as shown in Figure below.

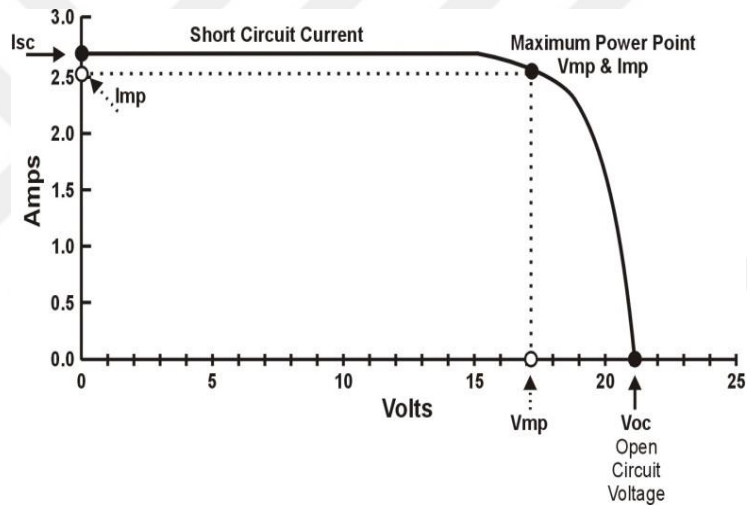


**Figure 2.9:** The I-V characteristic curve of a solar panel.

## 2.4 Applications of Solar Energy

The solar energy which is a combination of light and heat is produced by the rays of the sun. This energy moves from the sun and reaches to the earth where human collects it through the solar collectors and transfer it into any desirable form of energy. According to the hypothesis, this renewable energy source is powerful enough to replace the need of electricity that we get from 650 barrels of oil per year [19].

1. Power plant: In conventional power plants, nonrenewable energy sources are utilized to boil water and form steam so that it can rotate turbines and water to



produce electricity. But with the application of solar thermal energy, the sun can be applied to boil that water and to generate steam and rotate turbines. To convert the sunlight into electricity, the solar panels, thermal photovoltaic technologies and techniques etc. are used as shown in Figure (2.10) [19].

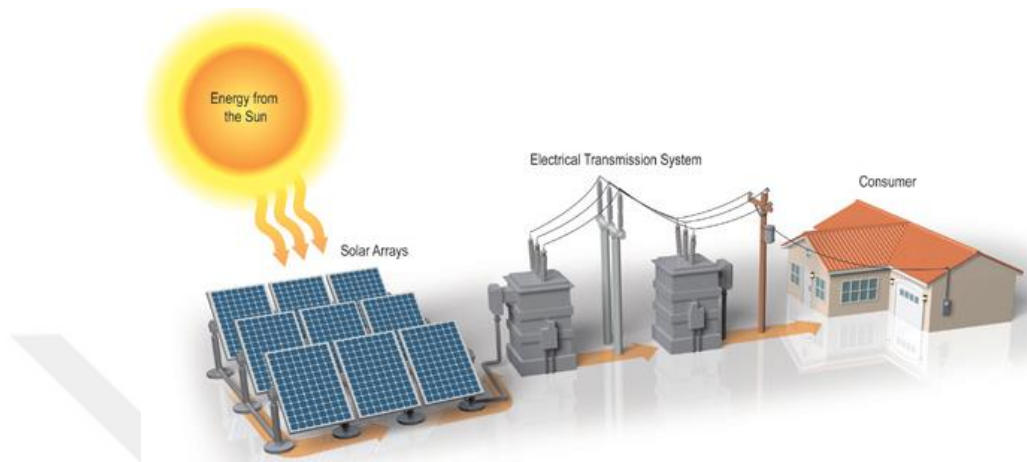


**Figure 2.10:** Photovoltaic panels in power plant.

2. Homes: utilize of solar energy is increasing at homes as well. The residential machines can readily utilize electricity generated by the solar power. This solar energy is operating the solar heater in order to provide hot water at homes. Still, the photovoltaic cell installed on the house roof as shown in Figure (2.11), the energy is grabbed and stocked on batteries to utilize during the day at homes for different applications. In this ways expense on energy is cutting down by home users [19].



**Figure 2.11:** Photovoltaic panels in homes.

3. Commercial use: on different buildings roofs, we can discover glass PV modules or any other type of solar panel. These panels are utilized to supply electrical power to various offices or other sections of building in a reliable method. These panels gather solar energy from sun, change it into electrical power and allow offices to utilize their own electricity for various purposes as shown in Figure (2.12) [19].



**Figure 2.12:** Photovoltaic panels for commercial usage.

4. Solar lighting: These lights shown in Figure (2.13) are also known as day lighting, and operate with assist of solar power. These lights stock the sunlight in day time and then transform the solar energy into electrical energy to turn it on during the night time. The utilization of this system is decreasing the load form on the local power stations [19].



**Figure 2.13:** The solar lighting.

## **2.5 Advantages of The Solar Energy**

Despite the cost compared to the other energy sources, the solar energy is attracting attention due to the following:

1. Solar energy makes use of renewable natural source that is readily available in many parts of the world.
2. The process used to generate solar energy is emission-free.
3. Technological progress has reduced costs to a point where it can compete with alternatives fossil fuels in specific circumstances.
4. The technology is scalable since it can be used for domestic heating applications or to generate commercial electricity scale more widely, as solar water heaters are well-established technology, available in a large scale and simple to install and maintain [20].

## **2.6 Obstacles of Spreading The Solar Energy**

The biggest obstacles to increase the solar power generation are the cost, the amount of land needed to produce large-scale electricity, and the intermittent nature of the needed energy source.

In terms of the latter, the thermal systems do not work at night or in adverse weather conditions. The hot water storage for domestic or commercial use is simple, it only required insulated tanks, but the higher-temperature liquids storage to produce large-scale electricity (or storage of the electricity itself) requires further technological development [20].

## **CHAPTER THREE**

### **METHODOLOGY AND PROPOSED PROTOTYPE**

#### **3.1 Introduction**

This chapter focuses on the design, program, and implementation of the proposed dual axis solar panel tracker system by using the Arduino Uno microcontroller.

The design will be done by using Proteus 8 simulation program; it will be implemented and tested practically. The Arduino Uno microcontroller is going to be programmed by using the Arduino C language.

#### **3.2 Drawing of The Mechanical Parts**

I draw the mechanical parts of the proposed dual axis solar panel tracking system by using AutoCAD 2017 program because it is considered as a main part for utilizing the PVC foam in the cutting machine (CNC), as described in the following steps:

1. Drawing the upper section as shown in Figure (3.1)

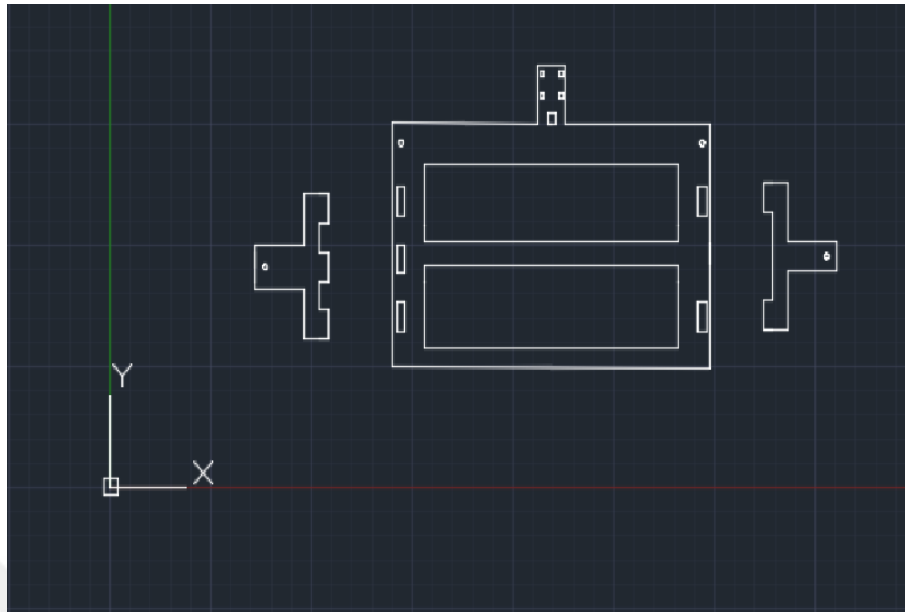


**Figure 3.1:** Parts of the upper section.

2. Drawing the middle section as shown in Figure (3.2)

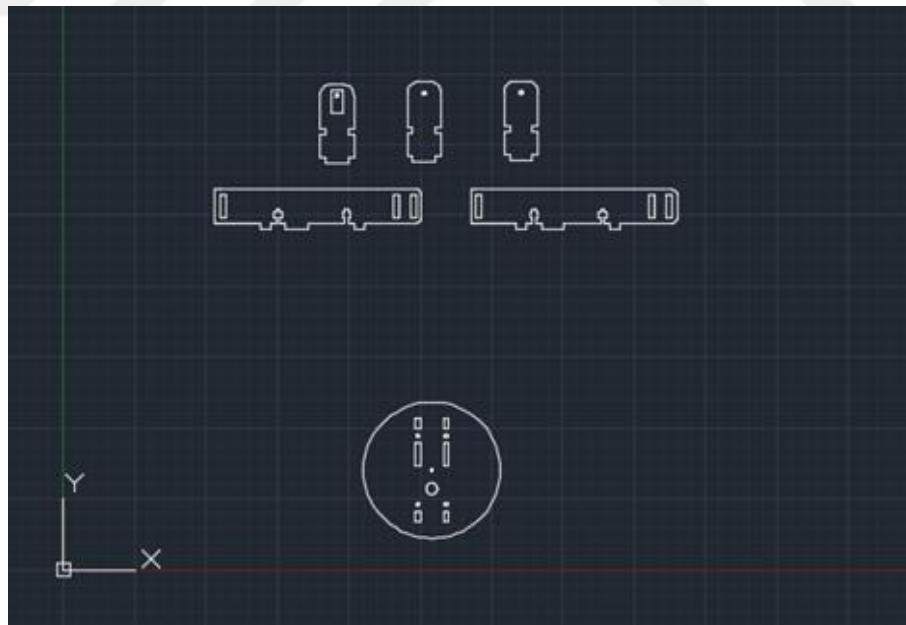


**Figure 3.2:** Parts of the middle section.

3. Drawing the lower section as shown in Figure (3.3)

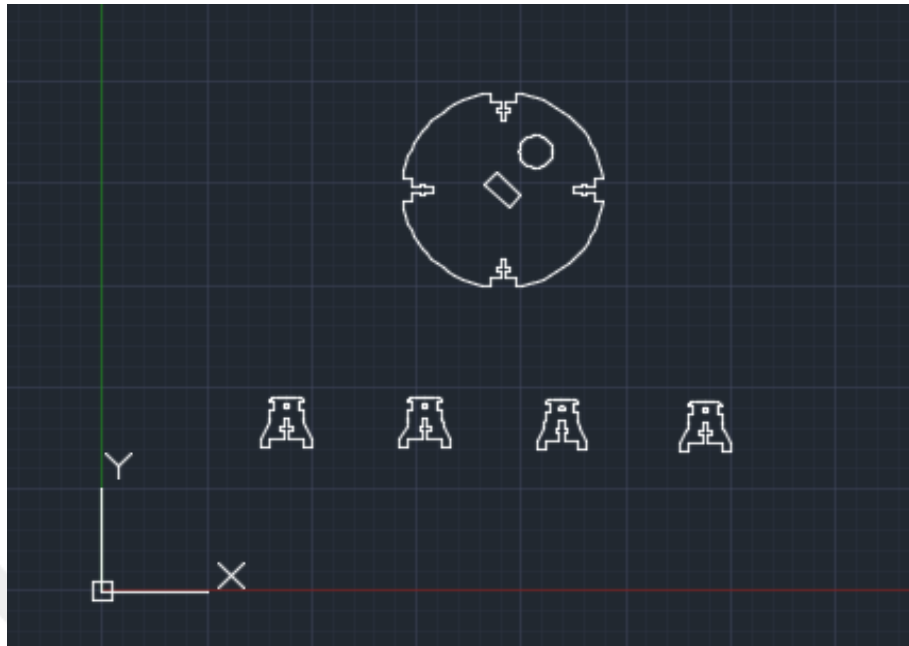


**Figure 3.3:** Parts of the lower section.

4. Drawing the base of the design as shown in Figure (3.4)

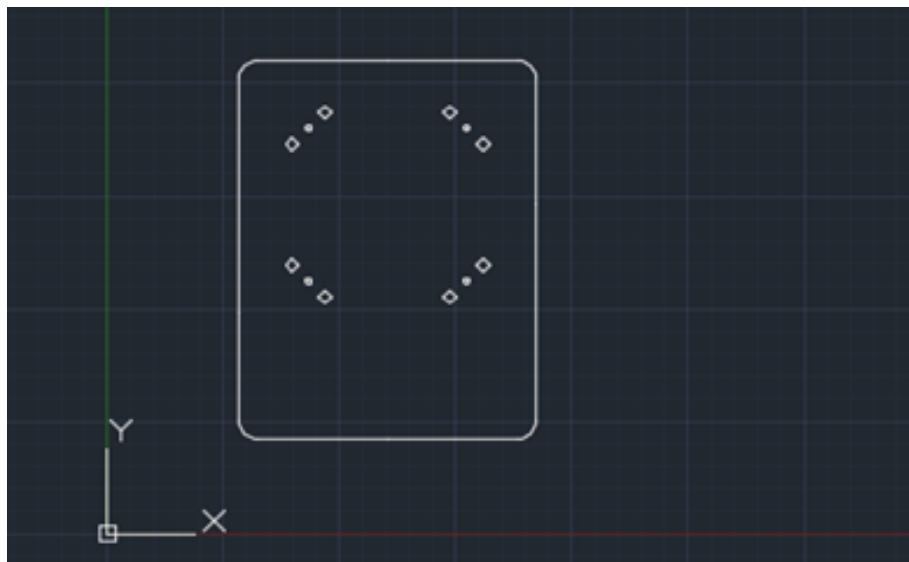


**Figure 3.4:** The base of the design.

### 3.3 Installation of The Mechanical Parts

By using the AutoCAD to draw the required pieces, I sent the commands and the drawings to the PVC foam cutting machine (CNC) in order to cut the required pieces as shown above. Later on, I put (Length: 1 meter) (Thickness: 1cm) from the PVC foam material under the (CNC) machine and turn on the cutting machine. Directly, the CNC started to cut according to my design, my drawings and my scales. Eventually, the (CNC) finished the cutting operation, and now; the pieces are ready to install in order to make a successful solar panel tracking system. The following steps show how the connection of the dual axis solar panel tracking system has done.

1. Connecting the parts of the lower section shown in Figure (3.5) is the most important section of the design because the weight of the design will be concentrated on this section. By using screwdriver and screws, I connected the horizontal motor at the center of the circle which is a part of the section. Then, I connected four legs on four sides of the circle in order to afford the heavy weight of the device after finishing the installation of the design. The four legs have been installed on the base of the design by using screws.

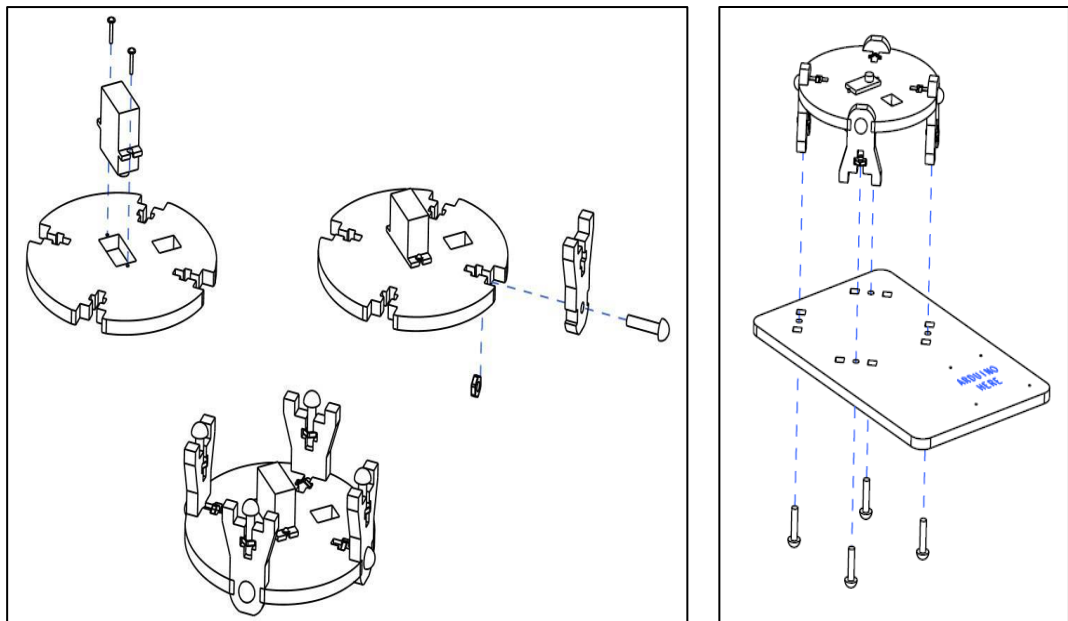
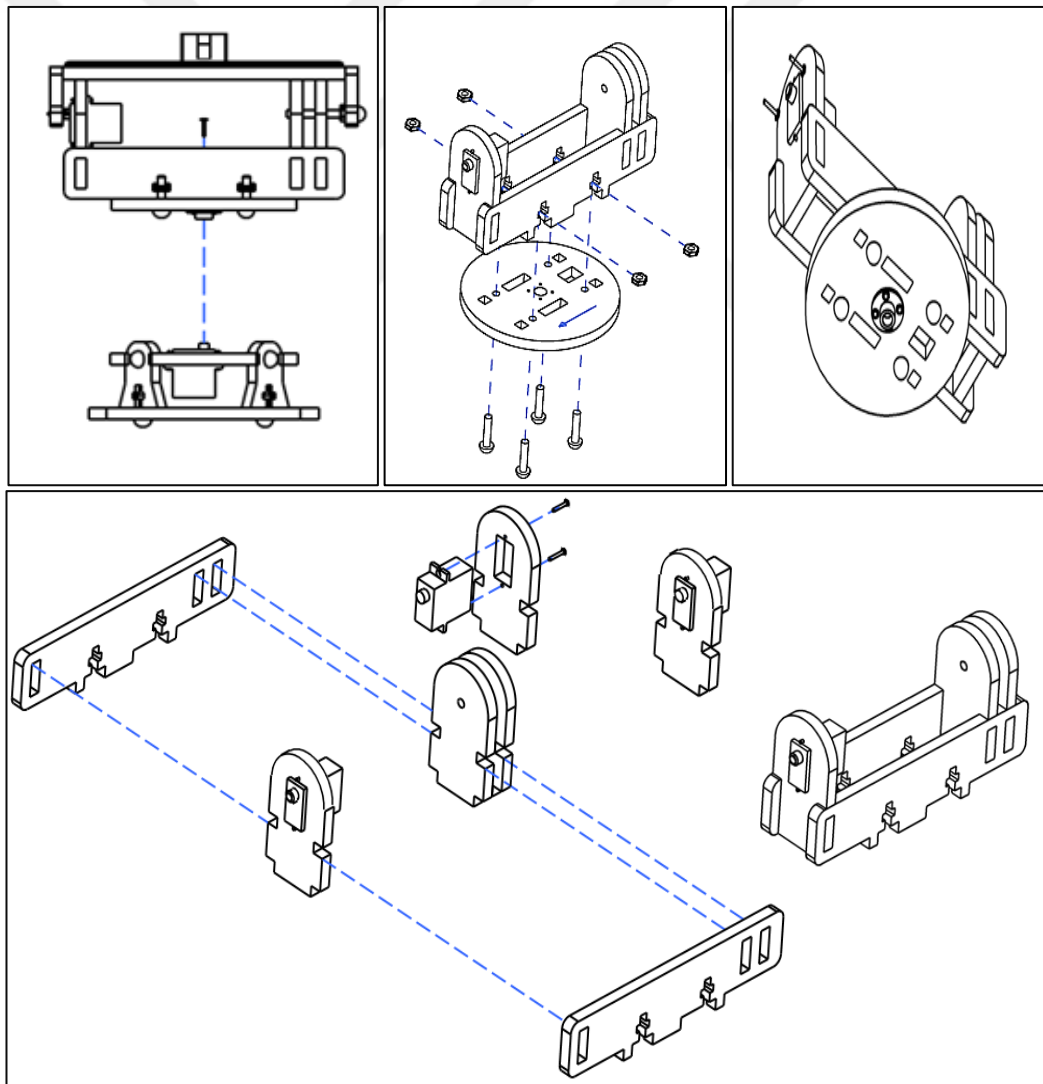


Figure 3.5: Connection of the lower section.

2. Connecting the parts of the middle section shown in Figure (3.6) is the first movable section of the device because it can move from east to west by connecting this section with the lower section of the design by using the horizontal servo motor. It works as a connector between the upper section and the lower section of the design. By using screwdriver and screws, I connected the vertical servo motor on the upper left side of this section in order to control the upper section of the design by using the vertical servo arm. I also used other supporters in order to fix this section. There is a circle at the lower part which contains slots on its surface in order to fix the supporters and the movable parts from the upper side, as well as I put a horizontal motor on the lower side to move the angle from east to west. At the end, the moving supporters of the upper section are connected on both sides of this section.



**Figure 3.6:** Connection of the middle section.



3. Connecting the parts of the upper section shown in Figure (3.7) is the second movable section of the design which connects the vertical servo arm of this section with the vertical servo motor of the middle section from one side and from the other side the right moving supporter of this section with the right supporter of the middle section to control the angles from North to South. Herein, I connected the solar cells (10 cells) in two cases (series and parallel). Then, I fixed the solar cells in the middle part by using the glue. Likewise, in the upper side, there are four slots for the LDRs which have square shapes. Finally, I used a piece of foam so as to insulate the four LDRs.

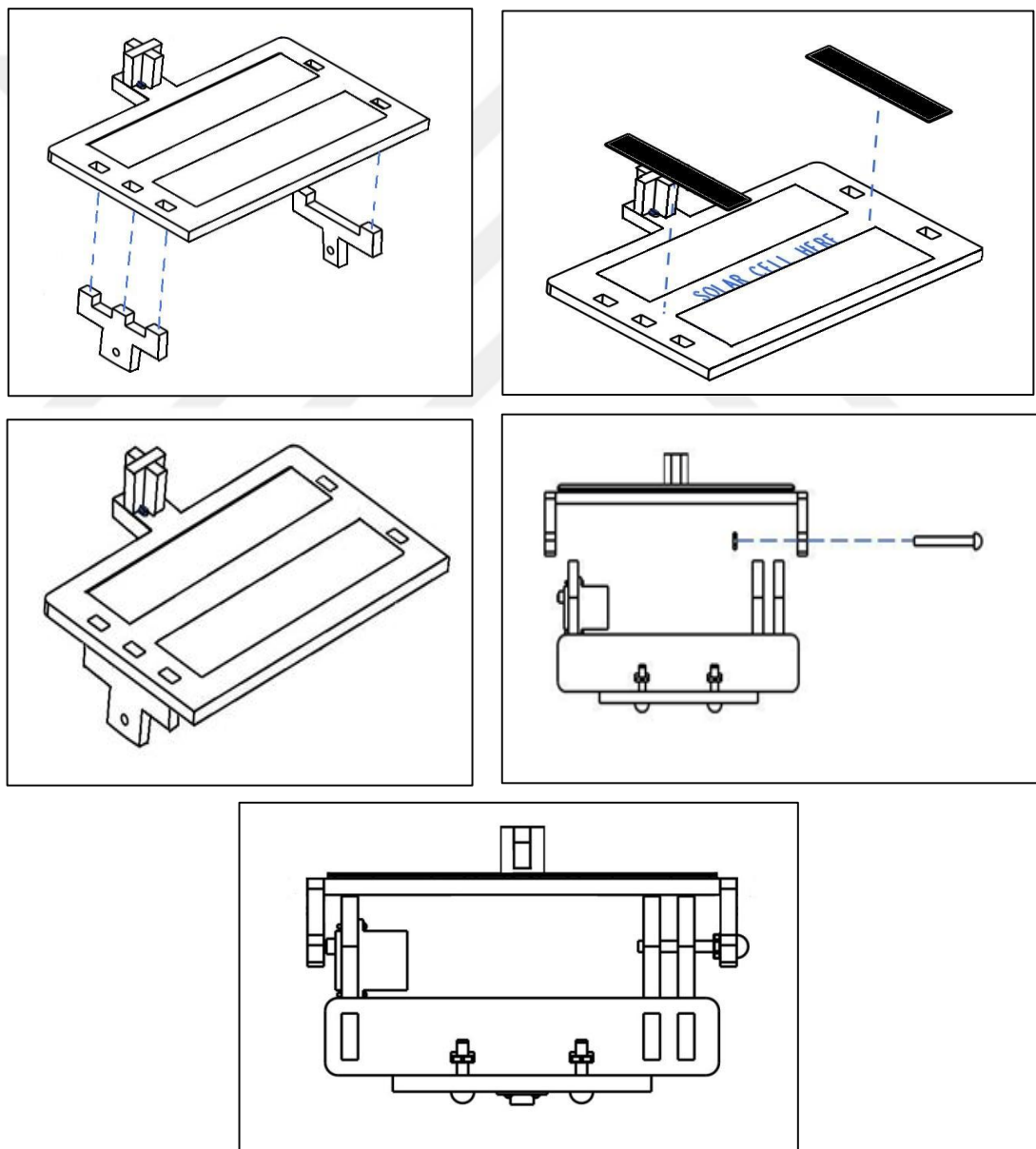


**Figure 3.7:** Connection of the upper section.

4. The final proposed prototype (mechanical part) is shown in Figure (3.8)

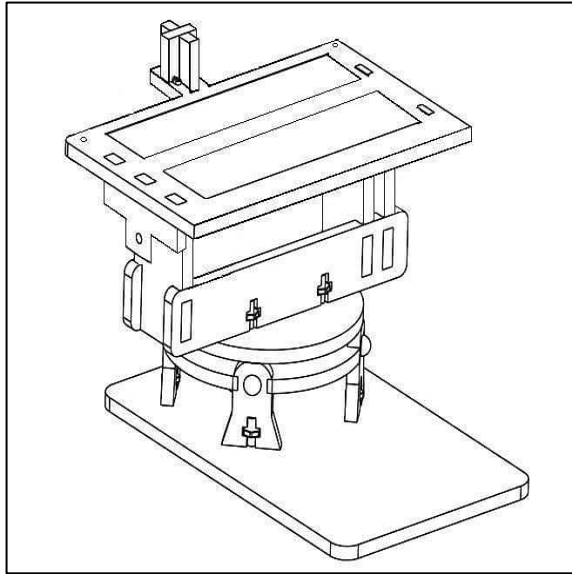


**Figure 3.8:** The final proposed prototype (mechanical portion).

### **3.4 Block Diagram**

The aim of the proposed dual axis solar panel tracking system is to keep the solar panel facing toward the sun all the day. Therefore, we have to track the position of the high intensity of the sunlight by using the LDRs.

The proposed design depends on the obtained value of the voltage difference between the four LDRs which are located in a shape of square on the upper section of the design. Automatically, the panel will rotate according to the obtained value. As shown below in figure (3.9), the proposed dual axis solar panel tracking system consists of the sensing unit, the microcontroller unit, and the two servo motors (rotation unit).

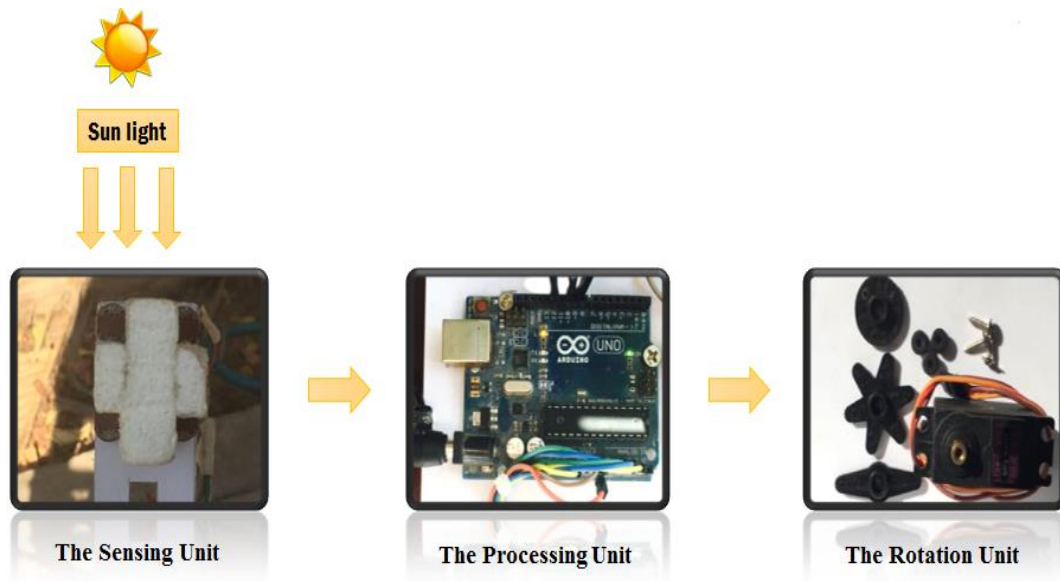


**Figure 3.9:** Block diagram of the proposed prototype.

### 3.5 Components of The Proposed Prototype

The components of the proposed solar panel tracking system are very sensitive. Therefore, it requires precision and concentration during the work. These components are electrical, electronic and mechanical. The proposed solar panel tracking system consists of two main circuits. The purpose of the first circuit is to sense the solar radiation by using LDRs, to control the Arduino Uno which is the brain of the design and to control the two servo motors (vertical and horizontal). The purpose of the second circuit which is the solar panel circuit is to convert the solar energy into electrical energy and to supply the electrical energy into the load.

#### 3.5.1 The Microcontroller Unit

Arduino Uno board shown in Figure (3.10) is the microcontroller and the brain of my design because it could be difficult to control any servo motor without using it. The Arduino Uno board is utilized herein since it can work independently or with the assistance of the computer. It receives analog signals from the LDRs by the analog pins and sends pulse width modulation signals (PWM) by the PWM digital pins to the two servo motors (horizontal and vertical). Therefore, regarding the voltage of this microcontroller unit, the Input voltage is (9V).

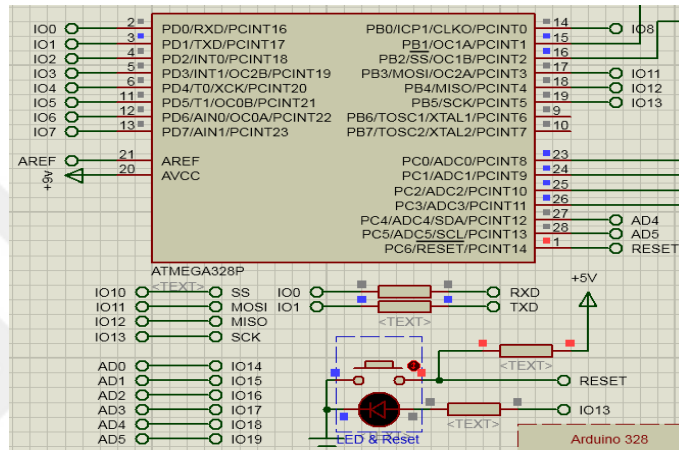
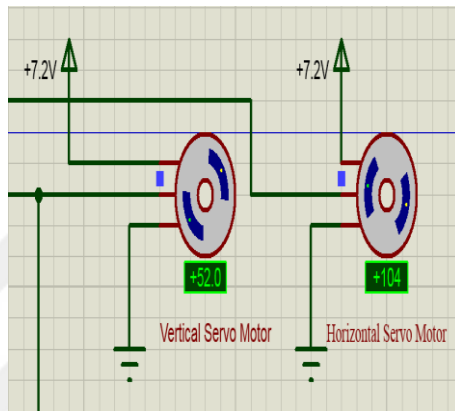
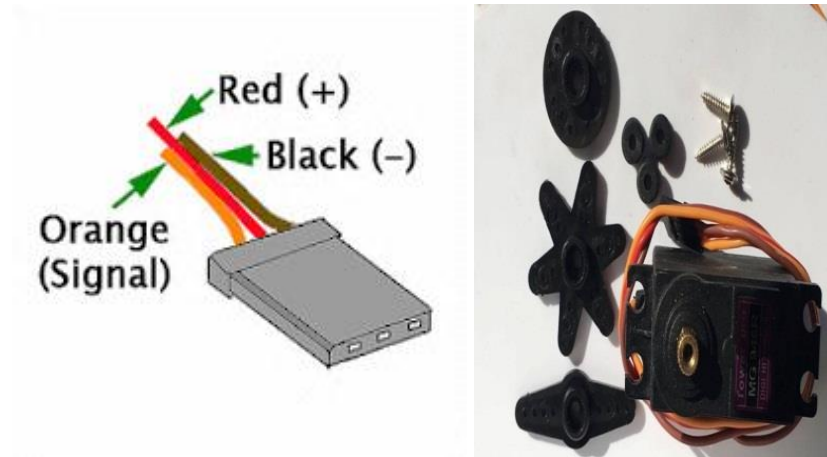


Figure 3.10: The simulation and working of the arduino uno board.

### 3.5.2 The Rotation Unit

Servo motor (MG 946R) shown in Figure (3.11) is the mechanical component of the proposed design. It has tough metal gears. I preferred this type of servo motors because it has high quality and high torque during the work of the solar panel tracking system. It has three main wires, the orange wire is for the pulse width modulation signal (PWM), the red wire is for the operating voltage (V+) and the last wire is for the ground as shown in Figure (3.11). There are two servo motors which are the horizontal and the vertical servo motors as shown in Figure (3.12). The horizontal servo motor controls the horizontal angle of the design (from east to west) while the vertical servo motor controls the vertical angle of the design (from south to north). Eventually, the operating voltage for the two servo motors is 7.2V.



**Figure 3.11:** The simulation and parts of the servo motors.

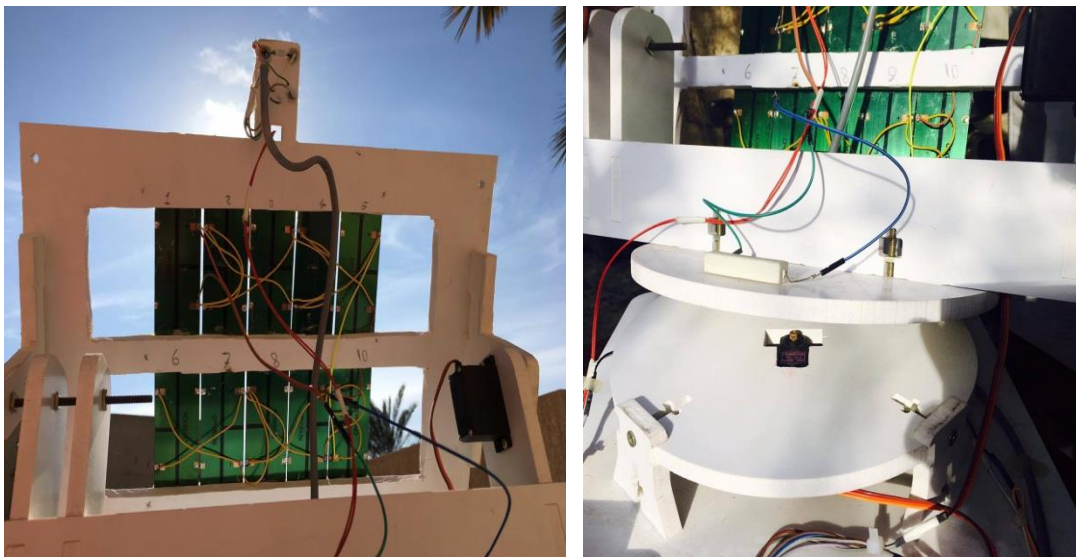


**Figure 3.12:** Vertical and horizontal servo motors practically.

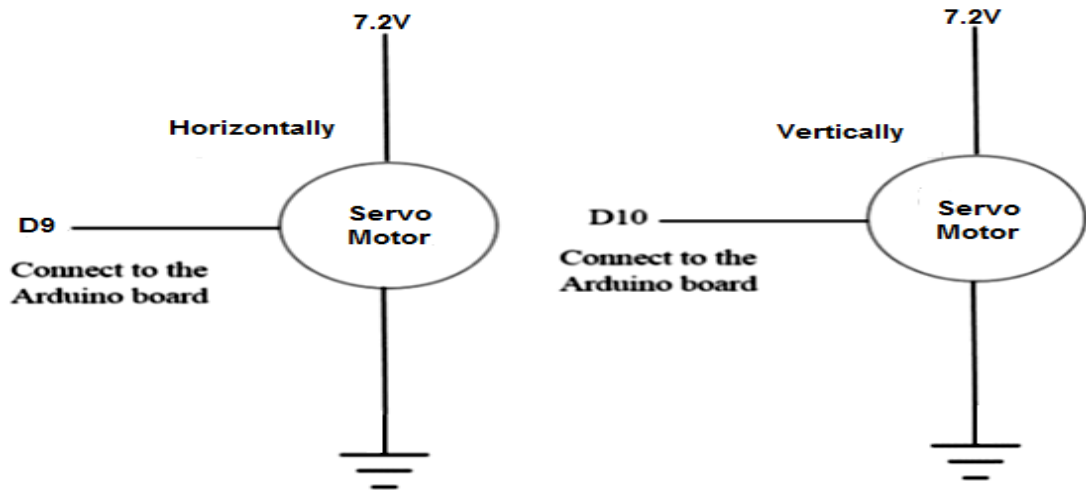


**Figure 3.13:** Servo motors connections to the Arduino Uno board.

### 3.5.3 The Sensing Unit

The light dependent resistor (LDR) shown in Figure (3.14) is the sensing part of the proposed design. In my thesis, this part can work as a light sensor to detect the absence and the presence of light. I chose them because they can cost a low price, as well as it has high sensitivity and simple structure. I put four LDRs in the upper section of the design in a shape of square. Directly as the (LDRs) sensing the light, they will give analog signals to the microcontroller. Moreover, the input voltage to the LDRs is 5V.

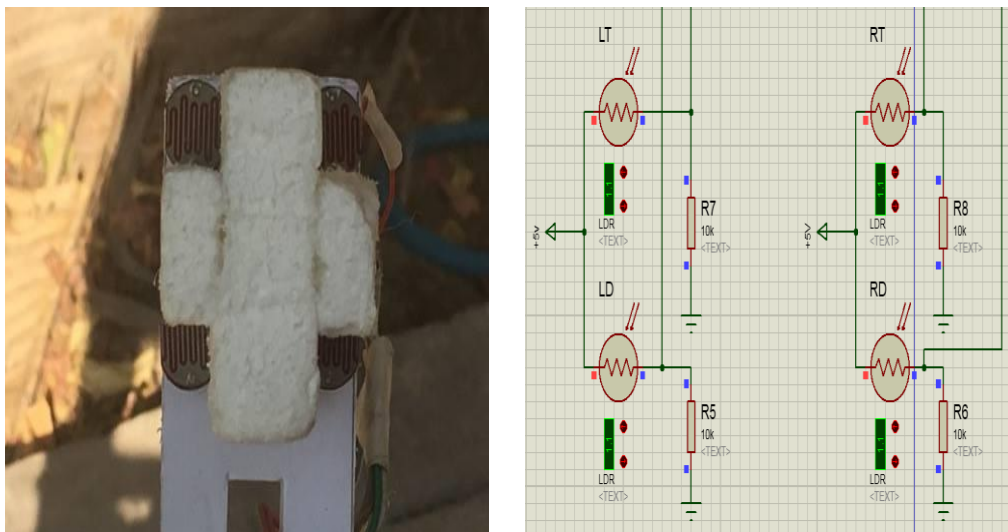


**Figure 3.14:** The simulation and position of the four LDRs.

The fixed resistors in Figure (3.15) are connected in series with the LDRs to form a potential divider circuit. The center point of the potential divider is fed to the analog pins of the Arduino board. In practical, I selected four fixed resistances in the proposed design and the value of each resistance is (360 $\Omega$ ).

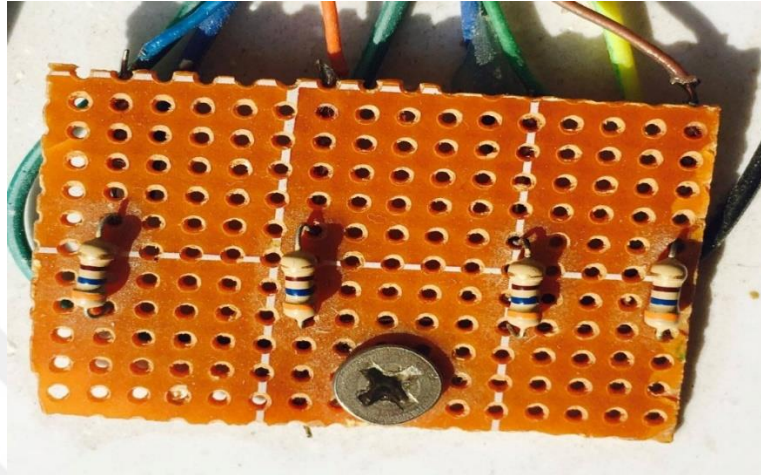


**Figure 3.15:** The fixed resistances (360 $\Omega$ ) practically.

### 3.5.4 Other Components

A. Voltage regulation (LM2596) shown in Figure (3.16) is a DC to DC step down regulation. I chose it because it is adjustable and ideal for the proposed design and I needed to step down the input voltage from 9V (adaptor) to 7.2V (servo motor voltage). I regulated the voltage from the adjustable part by using the screw driver and checked the voltage by using the AVO meter.

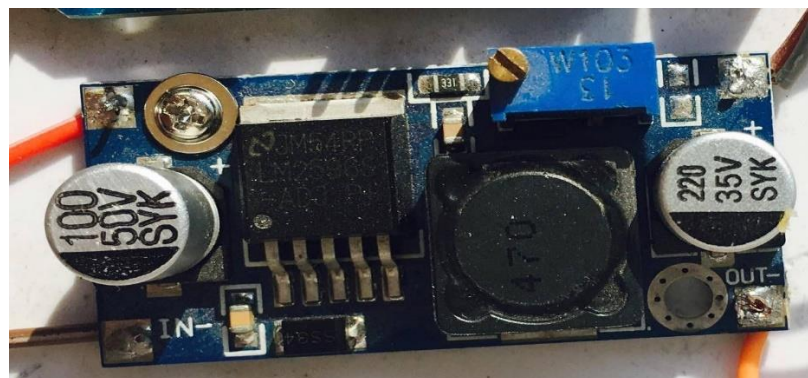


**Figure 3.16:** Voltage regulation LM2596.

Finally, there is not Voltage regulation LM2596 in PROTEUS 8.1. Therefore, instead, I used power terminal (+7.2V) in order to supply the two servo motors.

B. Thermometer shown in Figure (3.17) is used to measure the temperature of the solar panel. The unit of this part is °C. It is very accurate to the exact temperature. The input voltage for this part is 5V.



**Figure 3.17:** The thermometer.

C. Load for the proposed design: I chose a resistance (10W 300ΩJ) as a load which is connected with the solar cells (series or parallel case). The load voltage and the current depend on the solar energy absorbed by the solar panel. Eventually, I measured the output voltage and the current on both ends of this load by using the AVO meter as shown in Figure (3.18).

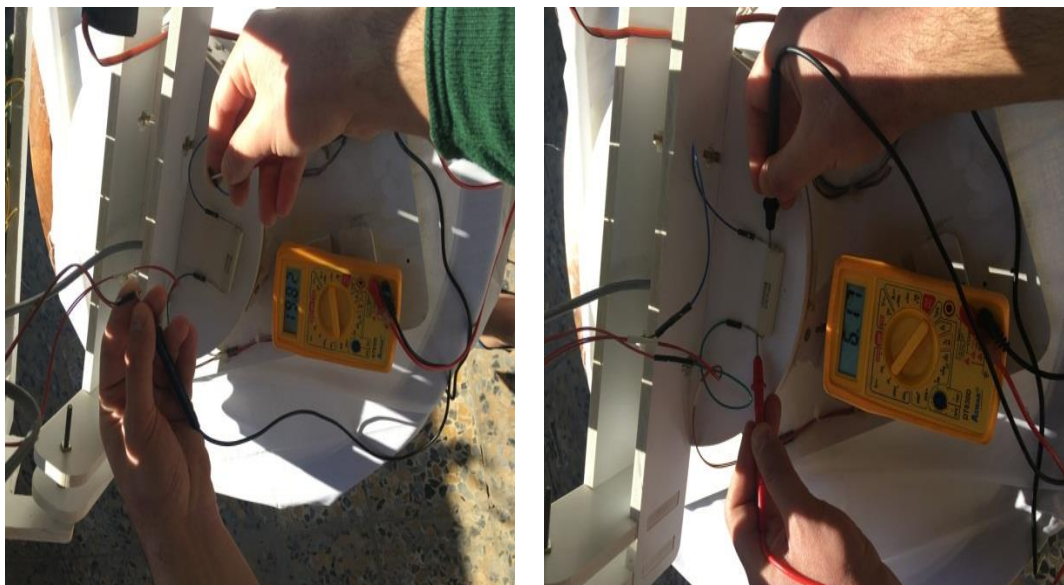


**Figure 3.18:** Load (10 W 300 ΩJ) with the measuring voltage and current.



D. 10 solar cells (6V 0.1W) in two cases (parallel and series connection) as shown in Figure (3.19) cost low prices and give high efficiency in absorbing the solar energy and converting it into electrical energy.

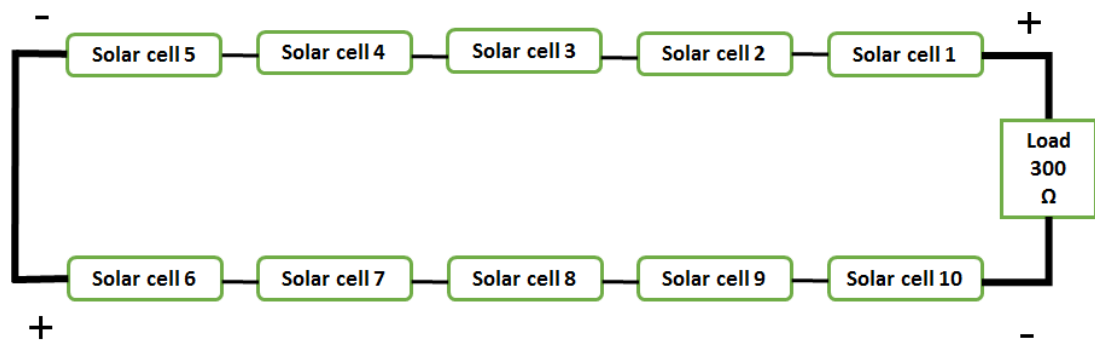


Figure 3.19: 10 solar cells.

Even though, the output power of the solar panel is quite small, but the solar panel is enough to show that the sunlight energy can be grabbed as much as possible because the solar panel is moving in response to the direction of sunlight that sensed by LDRs.

### 3.6 Solar Cells Connections

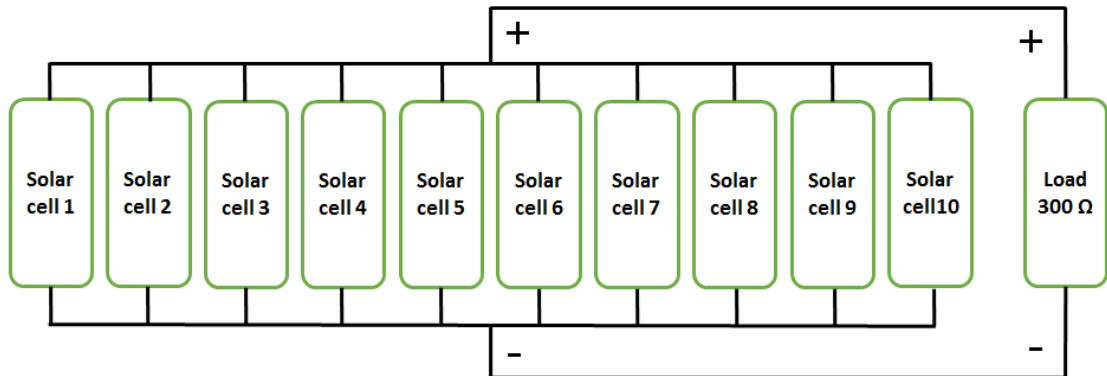
A. Series case: In this case shown in Figure (3.20), the load voltage will be more variable.



Solar Panel 15V 50mA 0.75W

Figure 3.20: Series solar cells connection.

B. Parallel case: In this case shown in Figure (3.21), the load voltage will be constant.



**Solar Panel 6V 50mA 0.12W**

**Figure 3.21:** Parallel solar cells connection.

### **3.7 Inputs and Outputs to The Arduino Uno Board**

A. Inputs: four LDRs are used in four different locations (up right, down right, up left and down left) to measure the intensity of the light. Arduino Uno board receives and reads the analog values of the LDRs.

B. Outputs: two servo motors are used as outputs of the Arduino to rotate the solar panel in different directions in order to get the maximum output power.

### **3.8 Simulation of The Proposed System**

In this work, we used Proteus 8.1 for simulation and for drawing the schematic of our circuit. Figure (3.22) shows the simulation of the proposed dual axis tracking system which already described in section 3.4.

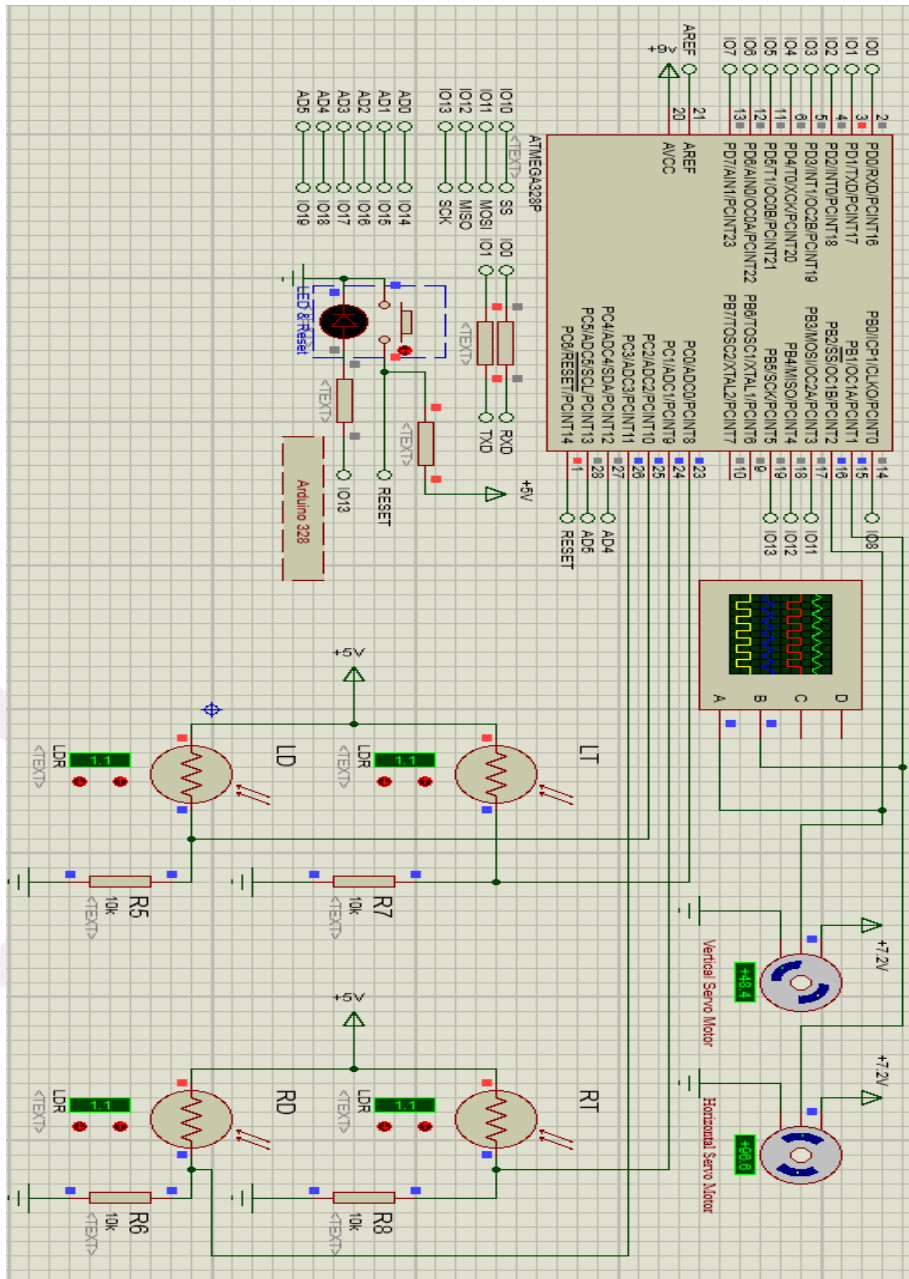


**Figure 3.22:** The completed simulation of the proposed tracking system.

It is clear from this figure that the 4 LDRs are connected to the analog input pins of the Arduino board A0, A1, A2 & A3. On the other side, the servo motors were connected to the digital output pins D10 & D9.

### 3.9 Working Principle of The Proposed System

When the sunlight falls on the LDRs, the microcontroller will sense the variation of light by the analog pins. We have 3 cases:

### Case 1

When the sun is located on the right or left or up or down the four LDRs, the voltage value will increase in the analog pins which are connected on the LDRs toward the sun and will decrease on the LDRs opposite to the sun. For example, if the sun is located on the right side of the four LDRs, the voltage value will increase in the right analog pins and will decrease in the left analog pins. Then, the microcontroller will calculate the average of the increasing voltage between the right up LDR and the right down LDR. Also, it will calculate the average of the decreasing voltage between the left up LDR and left down LDR. By applying the subtraction operation on the two resulting averages, the resulting value from the operation will take these results as commands to move the horizontal motor to the right direction and to equalize the voltages of the analog pins by equalizing the intensity of the sunlight on the LDRs. Moreover, for the other directions, we can apply the same operation in order to show the aimed results.

### Case2

When the sun is located on the right up or left up or right down or left down the four LDRs i.e. the effect of the sun will be in two directions (will not be in one direction). For example, if the sun is on the right up of the four LDRs, the LDR which is located on the right upside will be towards the sun and the voltage of this analog pin will increase. Contrastingly, regarding the sensor which is located on the opposite side to the sun (the left down sensor), the voltage of the connected analog pin will be lower than the other pins. Thus, when the microcontroller does the calculation, the right analog pins voltages will be increased and the upper analog pins voltages will also be increased. Moreover, the vertical servo motor will move up and the horizontal servo motor will move to the right till the voltages of the analog pins will be equalized. This process can be applied to the other directions to show the aimed results.

### Case 3

In the case of darkness or the same amount of the falling solar rays on the four LDRs, the voltages of the four analog pins will be equal and the microcontroller will command the 2 servo motors to stay in the same position (no motion).

### 3.10 The LDRs Resistance With Different Angles of The Sun

As we know, the resistances of the LDRs are very high in the normal case. But, when they absorb sunlight, they can drop dramatically. The measuring of the LDR resistance is shown in Figure (3.23).



Figure 3.23: Measuring the LDR resistance.

Table 3.1: The value of LDR resistance.

| Angle of the LDR | Value of the LDR resistance |
|------------------|-----------------------------|
| 0°               | 79.9Ω                       |
| 45°              | 140Ω                        |
| 90°              | 350Ω                        |
| 180°             | 500Ω                        |

Note that, the resistance of the LDR increases when the angle of the LDR is also increased as we have aforementioned in the previous table (3.1), when the LDR starts to be in the case of darkness.

### 3.11 Calculation of The Fixed Series Resistance

When the amount of the sunlight increases on the LDR, the LDR resistance and the voltage drop across the LDR resistance decrease while the voltage drop across the fixed resistance increases. The value of the fixed resistance depends on the supplied voltage and the purpose of the LDR. Let's discuss now the 2 cases of calculating the fixed series resistance:

Case 1

LDR resistance ( $r_1$ ) = 500  $\Omega$ .

Source voltage ( $V_s$ ) = 5 v.

Analog voltage input ( $V_{r2}$ ) = 2 v.

$$V_{r2} = \frac{r_2}{r_1 + r_2} * V_s$$

$$2 = \frac{r_2}{500 + r_2} * 5 \quad (\div 5)$$

$$\frac{2}{5} = \frac{r_2}{500 + r_2}$$

$$2r_2 + 1000 = 5r_2$$

$$3r_2 = 1000$$

$$r_2 = \frac{1000}{3} = 333.33 \text{ } \Omega.$$

Case 2

LDR resistance ( $r_1$ ) = 79.9  $\Omega$ .

Source voltage ( $V_s$ ) = 5 v.

Analog input voltage  $V_{r2}$  = 4 v.

$$V_{r2} = \frac{r_2}{r_1 + r_2} * V_s$$

$$4 = \frac{r_2}{r_1 + r_2} * 5 \quad (\div 5)$$

$$\frac{4}{5} = \frac{r_2}{79.9 + r_2}$$

$$319.6 + 4r_2 = 5r_2$$

$$r_2 = 319.6 \Omega.$$

From case 1 and case 2 we conclude that:

$r_2$  changes between  $333.33 \Omega$  and  $319.6 \Omega$  and from the standard table of the resistances we selected  $360 \Omega$  which is closed to  $333.33 \Omega$  and  $319.6 \Omega$ .

Where

$r_2$ : is the fixed resistance which is connected in series with the LDR.

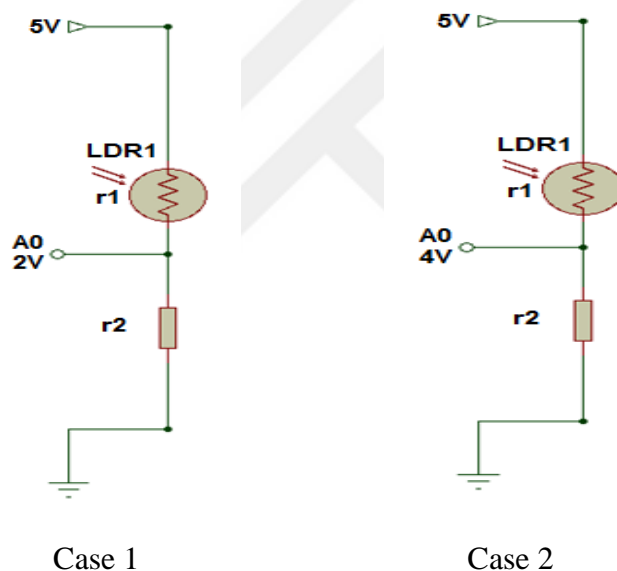


Figure 3.24: Cases of measuring the fixed series resistance.

### 3.12 Flowchart of The Tracking Operation

I programmed the Arduino board by using the Arduino C language to write the codes and command the Arduino C program (Personal Computer) to send these codes to the microcontroller board by using external cable. The Flowchart of our proposed design is shown in Figure (3.25).

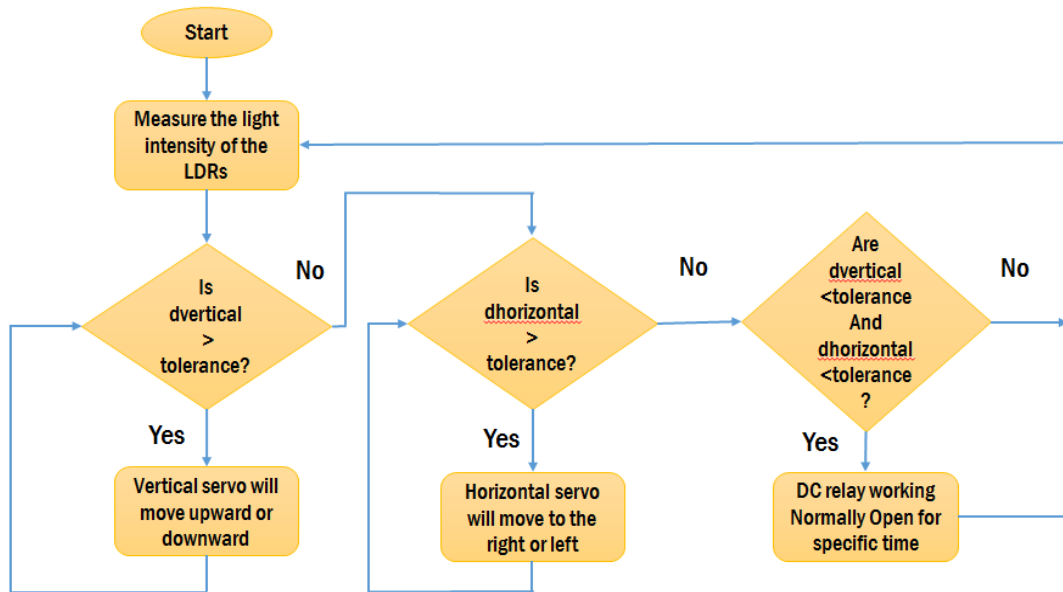


Figure 3.25: Flowchart of the tracking operation.

### 3.13 Our Final Prototype

The proposed dual axis solar panel tracking system, which has been practically achieved as mentioned in part 3.5, is shown in Figure (3.26).

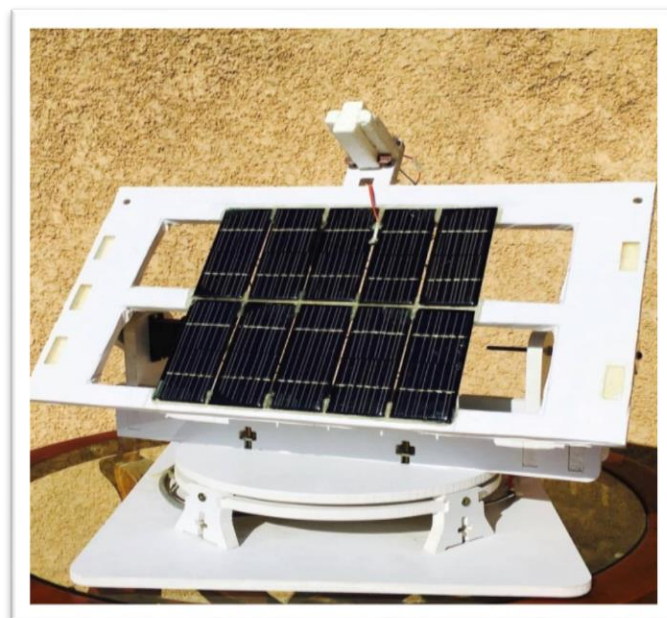


Figure 3.26: The proposed prototype.



## **CHAPTER FOUR**

### **RESULTS AND DISCUSSION**

In this chapter, we summarize the acquired results during our work. We start by comparing our prototype with another prototype developed by the department of electrical and electronic engineering in Baghdad University. This prototype was built for research purposes in Renewable energy laboratory and was made of iron, plastic and cements materials. Then, we will compare between the energy resulted from the static solar cells system and from the dual axis solar tracker by using ten solar cells of the same output power. We will discuss both cases: series and parallel connection. After that, we will show the results of the tracking and static systems of parallel case and calculate the average power. Then, we will display the energy values of the tracking and static prototypes of series case. The tracking system will be track the sun by switching the DC relay for an interval of time (5 mins, 10 mins, 15 mins, 20 mins, 30 mins, 40 mins, 50 mins, 55 mins, 1 hr, 2 hrs, 3 hrs, 4 hrs and 6 hrs) for a duration of 12 hrs while the static prototype will remain fixed toward the sun at 90 degree angle all the day. We will determine the energy consumption and generation of our prototype for all cases and through them we will calculate the efficiency.

The measurements have been done in Baghdad during the period from 10 to 31 august 2016, and the results were registered according to specific intervals of time from 6 am to 6 pm because sunrise in that period was between 5:21 and 5:35 am, whereas the sunset was between 18:53 and 18:28 pm.

#### **4.1 The Weight of Our Proposed Design**

We compared the weight of our prototype with a prototype built at the University of Baghdad in the laboratory of electrical and electronic engineering for

research experiments of student's research with the same specifications but made of iron, plastic and cement as shown in the figure (4.1) and compare the weight values of the prototypes illustrated in table (4.1).

**Table 4.1:** Comparison with reference prototype.

|                         | Proposed Design | Previous Design         |
|-------------------------|-----------------|-------------------------|
| Weight of The Prototype | 2.5 kg          | 4 kg                    |
| Material                | PVC Foam        | Iron + Plastic + Cement |

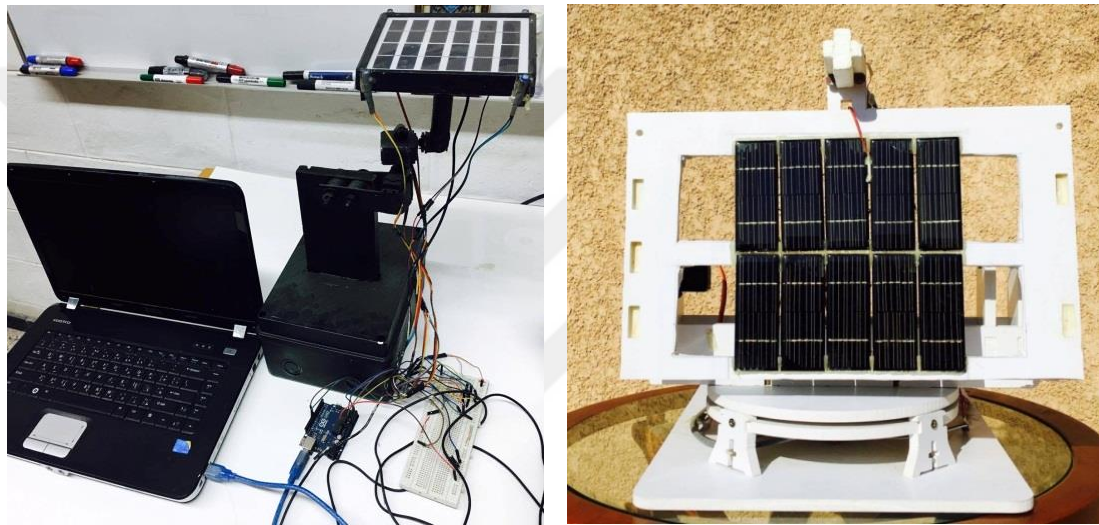


**Figure 4.1:** The reference prototype and our proposed prototype.

Therefore, the proposed design has less weight than the other design.

## 4.2 Results of Different Cells Connection Cases

We will display the results of the parallel case, then, we will also show the series case results in several cases.

### 4.2.1 Parallel Solar Cells Connection

We will connect ten solar cells in parallel to the load to calculate the average power value as shown in figure (4.2).

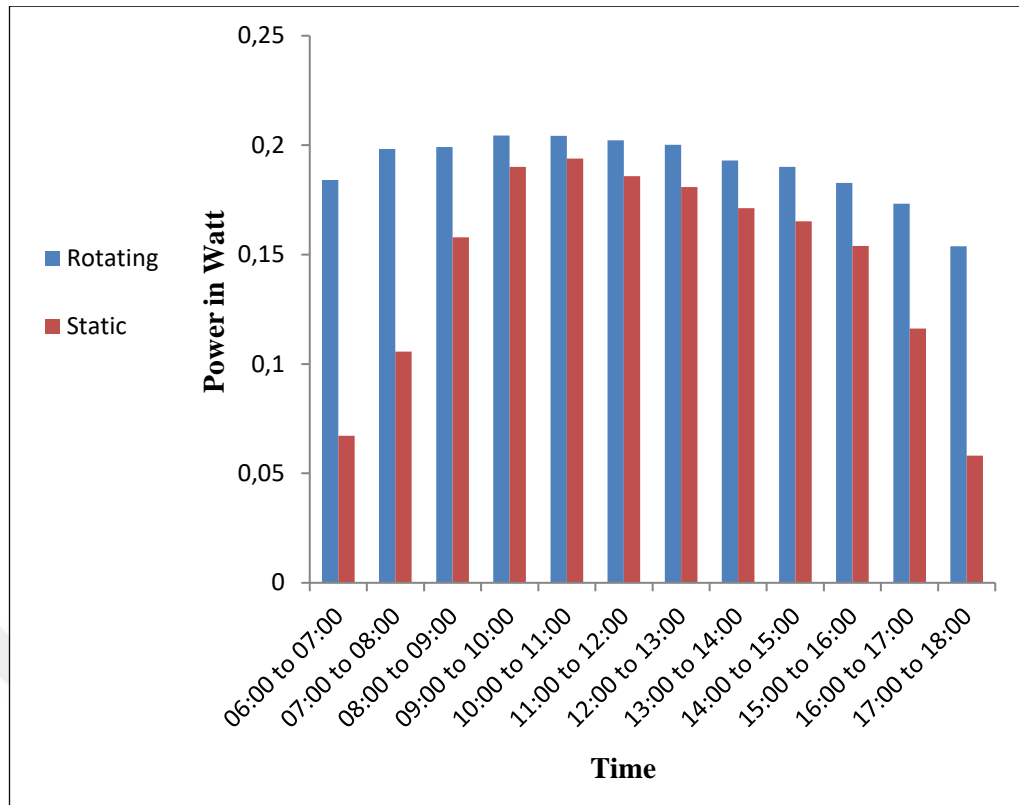


**Figure 4.2:** Interpretation data of power of solar panel 0.12 W.

Figure (4.2) demonstrates the data of power which are collected by static and rotating solar panels for the First day. The static solar panel data displays that the maximum power is 0.2045 W. For the meantime, the rotating solar panel data displays that the highest power is 0.1939 W. From figure (4.2), the power values produced by the rotating panel are approximately equal during the time of testing. But, for the static panel, it can be seen that the solar intensity increases from 06:00 to 07:00 until 09:00 to 10:00. Then, the solar intensity starts to decrease smoothly until at 17:00 to 18:00.

Figure (4.2) shows an increase in the total average power which is collected from the tracker solar panel in comparison to the total average power which is collected from the static solar panel.

#### 4.2.2 Series Solar Cells Connection

We will connect ten solar cells in series case to the load to calculate the average energy value by switching the DC relay for an interval of time (5 mins, 10

mins, 20 mins, 30 mins, 40 mins, 50 mins, 55 mins, 1 hr, 2 hrs, 3 hrs, 4 hrs and 6 hrs) for a duration of 12 hours.

#### 4.2.2.1 Switching DC relay using an interval of 5 minutes for 12 hours

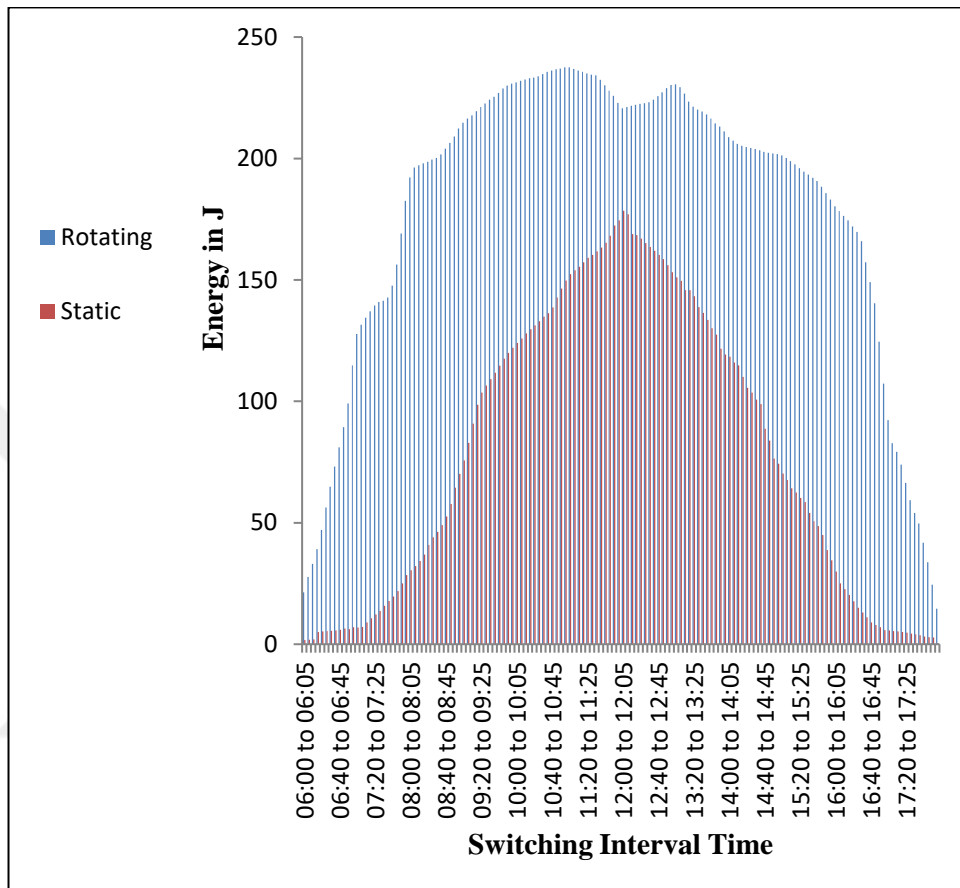


Figure 4.3: Rotating vs. static system for switching interval of 5 mins.

The results illustrated in figure (4.3) shows the obtained energy from the static and the tracker panels. By using the tracking system, the maximum energy was 237.4682 J could be reached from 10:55 to 11:05. Contrastively, without using the solar tracking system (static system), the maximum energy reached from 12:00 to 12:05 is 178.47 J. Also, the obtained energy of the tracker panel at any other time period is more than the obtained energy of the static panel at the same period.

Figure (4.3) also shows an increase in the total average energy which is collected from the tracker solar panel in comparison with the total average energy collected from the static solar panel.

Calculating the area under the envelope of the generated energy curve for the solar tracking system gives us the total average energy ( $E_t$ ) = 25871.50 J/ Day. As

a result, the total average energy obtained from the solar tracking system that follow the sun by interval of 5 minutes for 12 hours is equal to  $25871.50 - 10760.94 = 15110.56$  J/Day. On the other hand, the total average of the generated energy from the solar static system ( $E_s$ ) is equal to 11322.85 J/Day.

So, we can define the efficiency of our prototype by:

$$\text{The efficiency \%} = \frac{E_t - E_s}{E_s} * 100\% \dots\dots\dots (4.1)$$

Where  $E_t$ : The total average generated energy by the tracking system.

$E_s$ : The total average generated energy by the static system.

Using the equation (4.1), the efficiency of our system by using switching interval of 5 minutes is 33.45%.

#### 4.2.2.2 Switching DC relay using an interval of 10 minutes for 12 hours

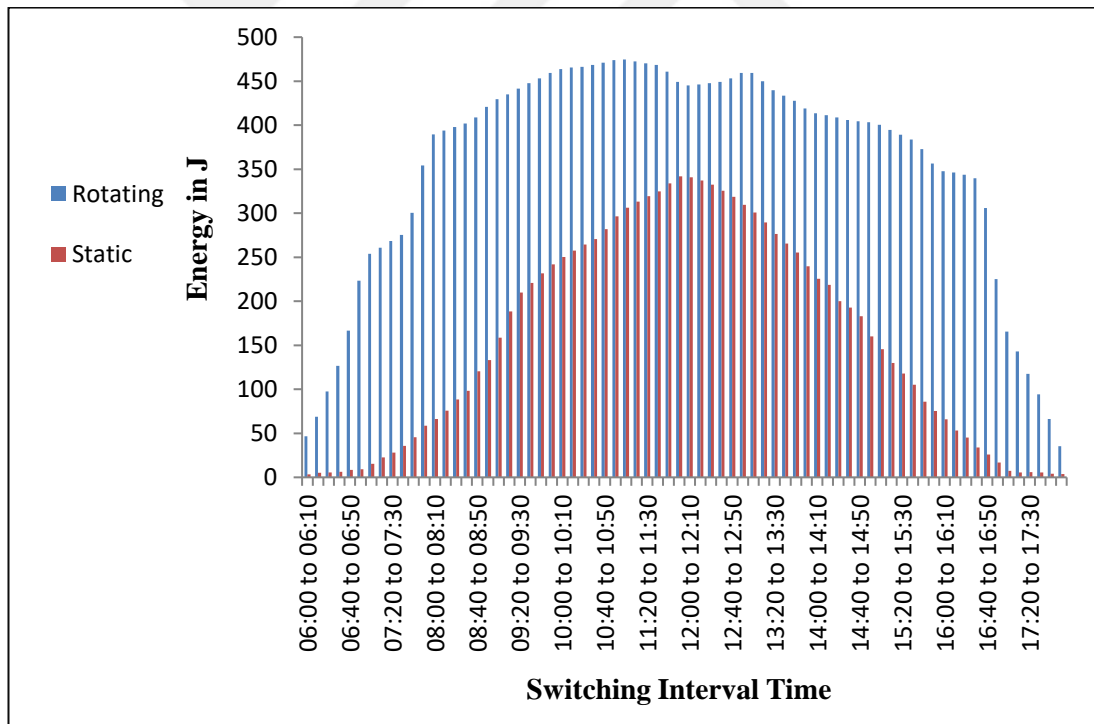


Figure 4.4: Rotating vs. static system for switching interval of 10 mins.

The results illustrated in figure (4.4) shows the obtained energy from the static and the tracker panels. By using the tracking system, the maximum energy was 474.63 J could be reached from 11:00 to 11:10. Contrastively, without using the solar

tracking system (static system), the maximum energy reached from 11:50 to 12:00 is 341.76 J. Also, the obtained energy of the tracker panel at any other time period is more than the obtained energy of the static panel at the same period.

Figure (4.4) also shows an increase in the total average energy which is collected from the tracker solar panel in comparison with the total average energy collected from the static solar panel.

Calculating the area under the envelope of the generated energy curve for the solar tracking system gives us the total average energy ( $E_t$ ) = 25731.12 J/ Day. As a result, the total average energy obtained from the solar tracking system that follow the sun by interval of 10 minutes for 12 hours is equal to  $25731.12 - 10611.9 = 15119.22$  J/Day. On the other hand, the total average of the generated energy from the solar static system ( $E_s$ ) is equal to 11322.85 J/Day.

Using the equation (4.1), the efficiency of our system by using switching interval of 10 minutes is 33.5%.

#### 4.2.2.3 Switching DC relay using an interval of 20 minutes for 12 hours

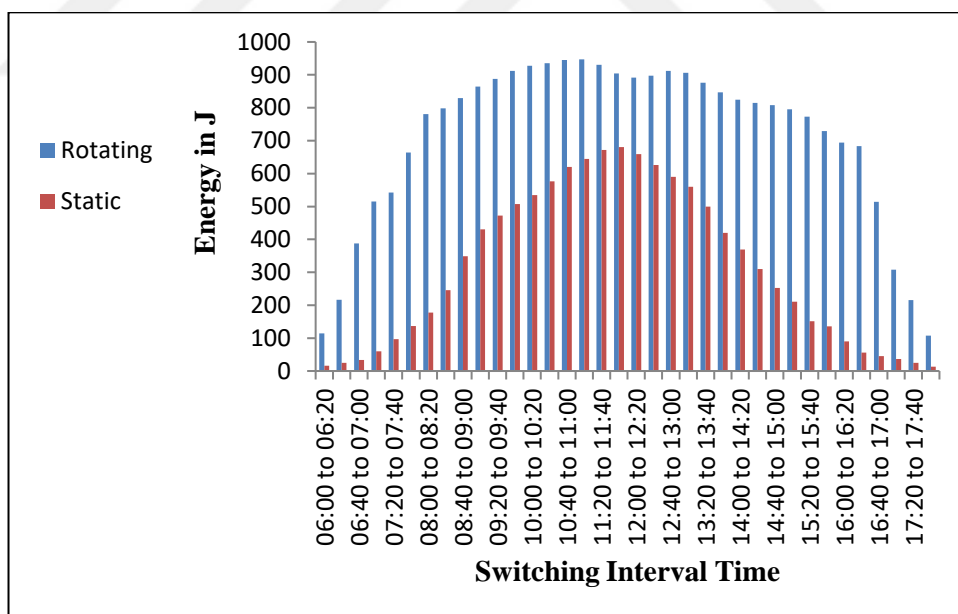


Figure 4.5: Rotating vs. static system for switching interval of 20 mins.

The results illustrated in figure (4.5) shows the obtained energy from the static and the tracker panels. By using the tracking system, the maximum energy was 946.8 J could be reached from 11:00 to 11:20. Contrastively, without using the solar tracking system (static system), the maximum energy reached from 11:40 to 12:00 is

680.4 J. Also, the obtained energy of the tracker panel at any other time period is more than the obtained energy of the static panel at the same period.

Figure (4.5) also shows an increase in the total average energy which is collected from the tracker solar panel in comparison with the total average energy collected from the static solar panel.

Calculating the area under the envelope of the generated energy curve for the solar tracking system gives us the total average energy ( $E_t$ ) = 25703.16 J/ Day. As a result, the total average energy obtained from the solar tracking system that follow the sun by interval of 20 minutes for 12 hours is equal to  $25703.16 - 10537.38 = 15165.78$  J/Day. On the other hand, the total average of the generated energy from the solar static system ( $E_s$ ) is equal to 11322.85 J/Day.

Using the equation (4.1), the efficiency of our system by using switching interval of 20 minutes is 34%.

#### 4.2.2.4 Switching DC relay using an interval of 30 minutes for 12 hours

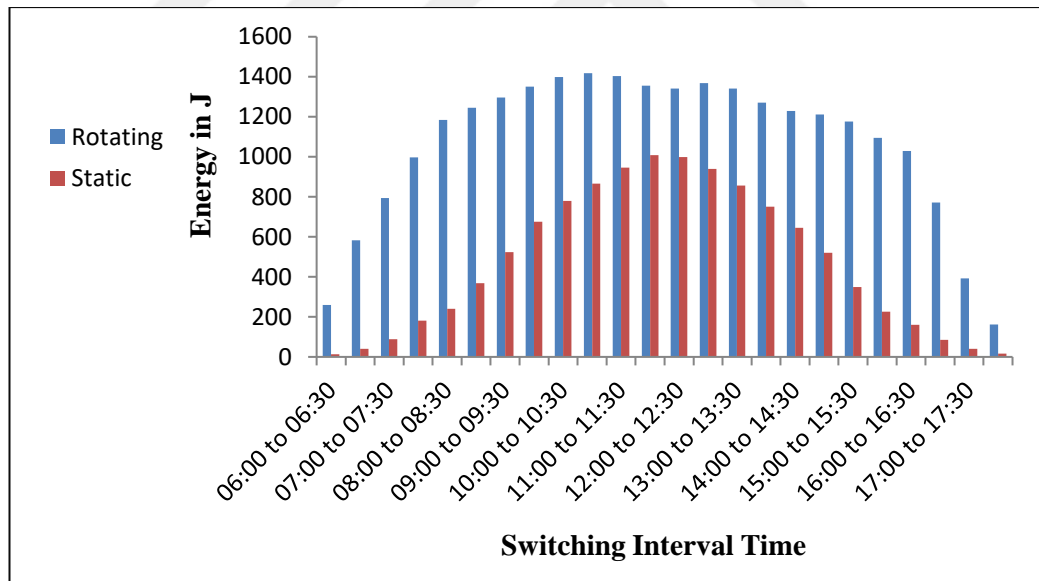


Figure 4.6: Rotating vs. static system for switching interval of 30 mins.

The results illustrated in figure (4.6) shows the obtained energy from the static and the tracker panels. By using the tracking system, the maximum energy was 1417.95 J could be reached from 10:30 to 11:00. Contrastively, without using the solar tracking system (static system), the maximum energy reached from 11:30 to

12:00 is 1007.91 J. Also, the obtained energy of the tracker panel at any other time period is more than the obtained energy of the static panel at the same period.

Figure (4.6) also shows an increase in the total average energy which is collected from the tracker solar panel in comparison with the total average energy collected from the static solar panel.

Calculating the area under the envelope of the generated energy curve for the solar tracking system gives us the total average energy ( $E_t$ ) = 25667.46 J/ Day. As a result, the total average energy obtained from the solar tracking system that follow the sun by interval of 30 minutes for 12 hours is equal to  $25667.46 - 10512.54 = 15154.92$  J/Day. On the other hand, the total average of the generated energy from the solar static system ( $E_s$ ) is equal to 11322.85 J/Day.

Using the equation (4.1), the efficiency of our system by using switching interval of 30 minutes is 33.8%.

#### 4.2.2.5 Switching DC relay using an interval of 40 minutes for 12 hours

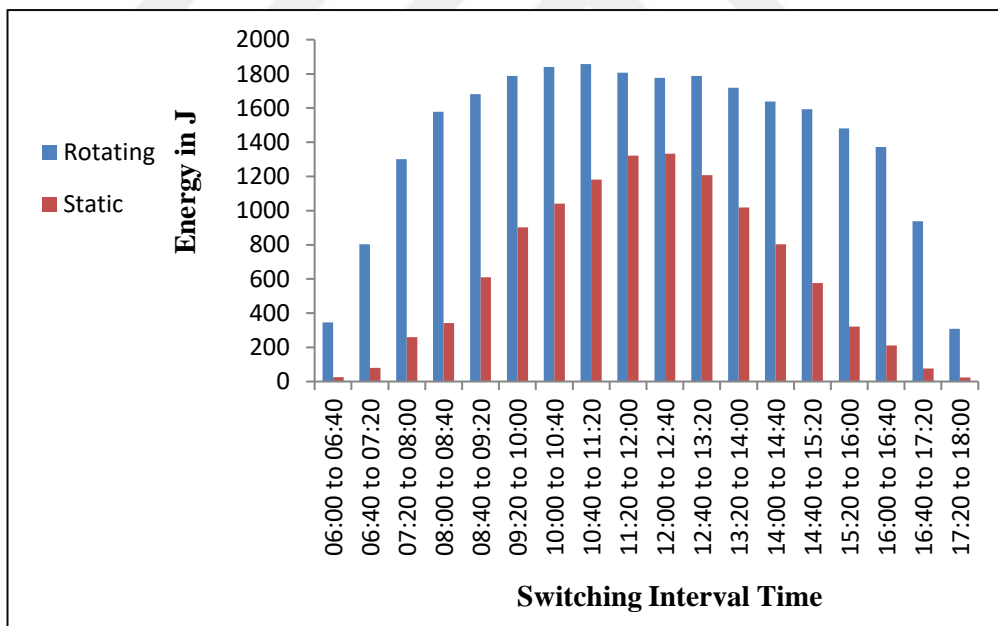


Figure 4.7: Rotating vs. static system for switching interval of 40 mins.

The results illustrated in figure (4.7) shows the obtained energy from the static and the tracker panels. By using the tracking system, the maximum energy was 1857.974 J could be reached from 10:40 to 11:20. Contrastively, without using the solar tracking system (static system), the maximum energy reached from 12:00 to



12:40 is 1332.6 J. Also, the obtained energy of the tracker panel at any other time period is more than the obtained energy of the static panel at the same period.

Figure (4.7) also shows an increase in the total average energy which is collected from the tracker solar panel in comparison with the total average energy collected from the static solar panel.

Calculating the area under the envelope of the generated energy curve for the solar tracking system gives us the total average energy ( $E_t$ ) = 25619.62 J/ Day. As a result, the total average energy obtained from the solar tracking system that follow the sun by interval of 40 minutes for 12 hours is equal to  $25619.62 - 10500.12 = 15119.5$  J/Day. On the other hand, the total average of the generated energy from the solar static system ( $E_s$ ) is equal to 11322.85 J/Day.

Using the equation (4.1), the efficiency of our system by using switching interval of 40 minutes is 33.53%.

#### 4.2.2.6 Switching DC relay using an interval of 50 minutes for 12 hours

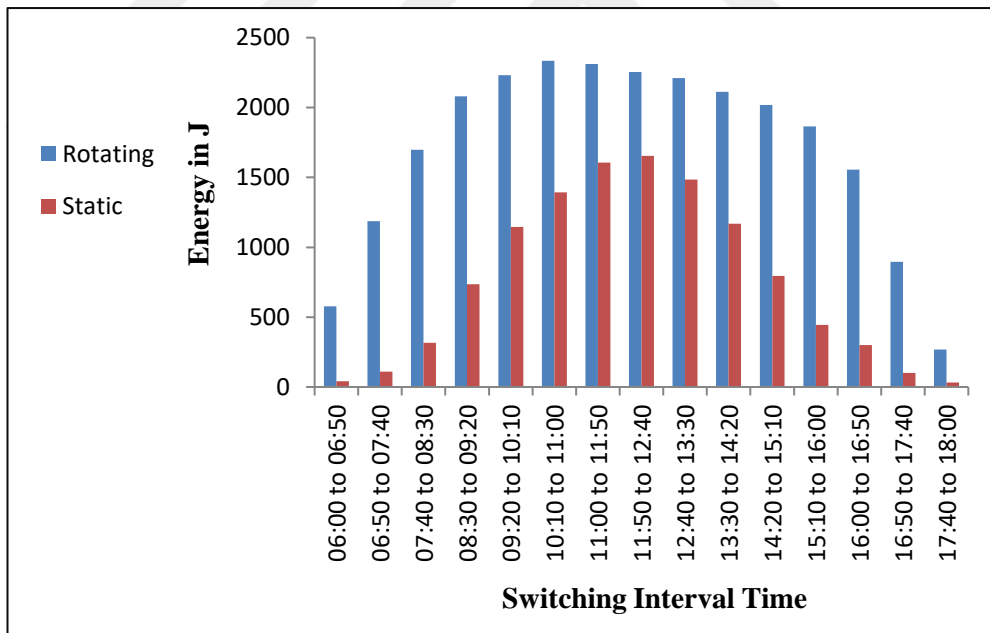


Figure 4.8: Rotating vs. static system for switching interval of 50 mins.

The results illustrated in figure (4.8) shows the obtained energy from the static and the tracker panels. By using the tracking system, the maximum energy was 2334.742 J could be reached from 10:10 to 11:00. Contrastively, without using the solar tracking system (static system), the maximum energy reached from 11:50 to

12:40 is 1654.65 J. Also, the obtained energy of the tracker panel at any other time period is more than the obtained energy of the static panel at the same period.

Figure (4.8) also shows an increase in the total average energy which is collected from the tracker solar panel in comparison with the total average energy collected from the static solar panel.

Calculating the area under the envelope of the generated energy curve for the solar tracking system gives us the total average energy ( $E_t$ ) = 25601.48 J/ Day. As a result, the total average energy obtained from the solar tracking system that follow the sun by interval of 50 minutes for 12 hours is equal to  $25601.48 - 10492.67 = 15108.81$  J/Day. On the other hand, the total average of the generated energy from the solar static system ( $E_s$ ) is equal to 11322.85 J/Day.

Using the equation (4.1), the efficiency of our system by using switching interval of 50 minutes is 33.44%.

#### 4.2.2.7 Switching DC relay using an interval of 55 minutes for 12 hours

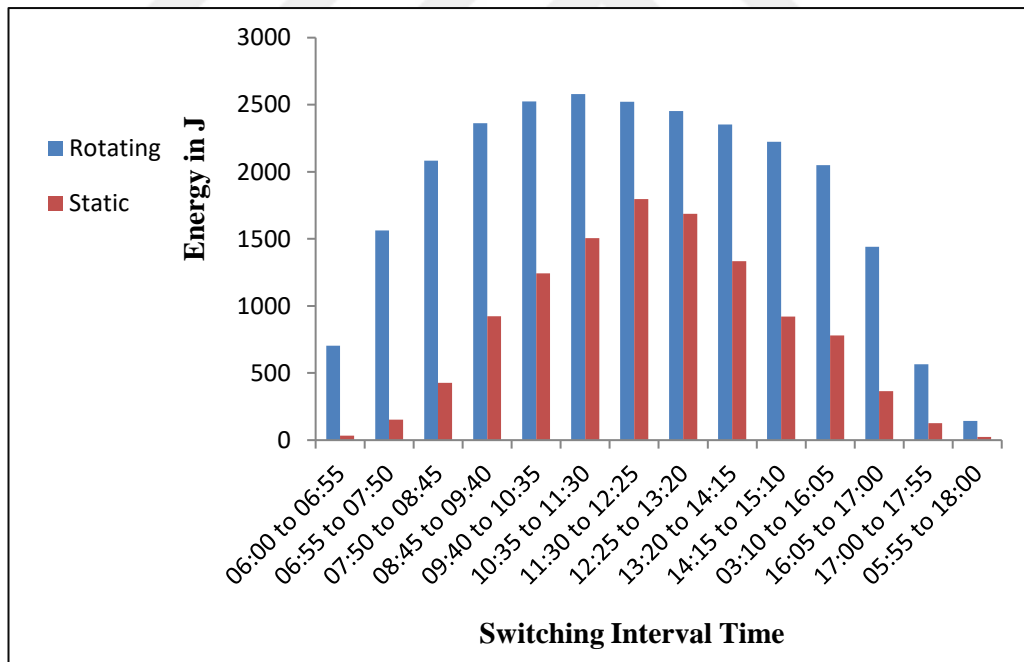


Figure 4.9: Rotating vs. static system for switching interval of 55 mins.

The results illustrated in figure (4.9) shows the obtained energy from the static and the tracker panels. By using the tracking system, the maximum energy was 2579.201 J could be reached from 10:35 to 11:30. Contrastively, without using the solar tracking system (static system), the maximum energy reached from 11:30 to

12:25 is 1796.685 J. Also, the obtained energy of the tracker panel at any other time period is more than the obtained energy of the static panel at the same period.

Figure (4.9) also shows an increase in the total average energy which is collected from the tracker solar panel in comparison with the total average energy collected from the static solar panel.

Calculating the area under the envelope of the generated energy curve for the solar tracking system gives us the total average energy ( $E_t$ ) = 25569.47 J/Day. As a result, the total average energy obtained from the solar tracking system that follow the sun by interval of 55 minutes for 12 hours is equal to  $25569.47 - 10489.96 = 15079.51$  J/Day. On the other hand, the total average of the generated energy from the solar static system ( $E_s$ ) is equal to 11322.85 J/Day.

Using the equation (4.1), the efficiency of our system by using switching interval of 55 minutes is 33.18%.

#### 4.2.2.8 Switching DC relay using an interval of 1 hour for 12 hours

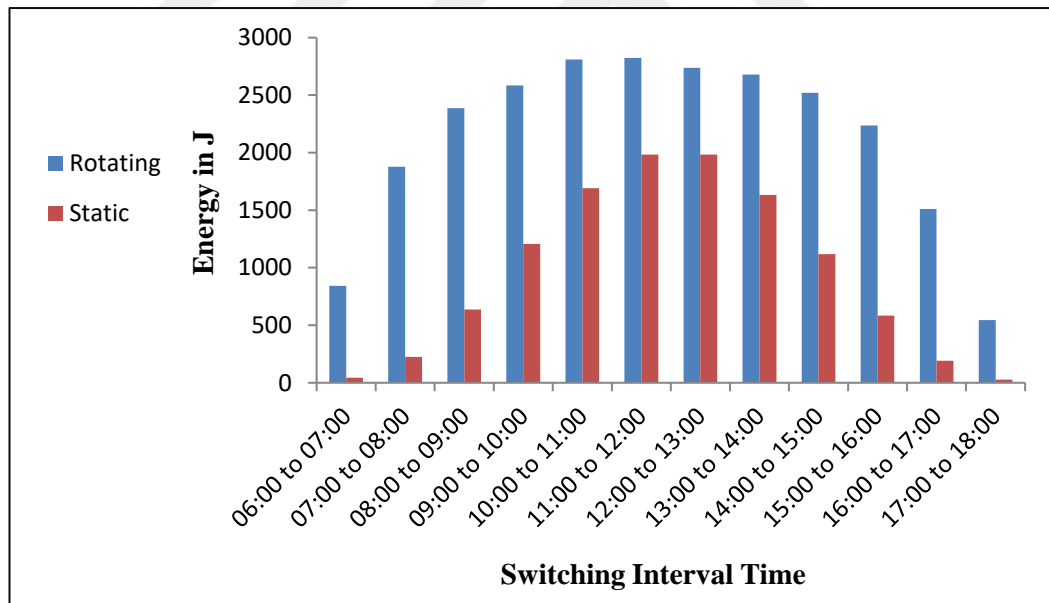


Figure 4.10: Rotating vs. static system for switching interval of 1 hr.

The results illustrated in figure (4.10) shows the obtained energy from the static and the tracker panels. By using the tracking system, the maximum energy was 2823.3 J could be reached from 11:00 to 12:00. Contrastively, without using the solar tracking system (static system), the maximum energy reached from 12:00 to 13:00 is

1984.662 J. Also, the obtained energy of the tracker panel at any other time period is more than the obtained energy of the static panel at the same period.

Figure (4.10) also shows an increase in the total average energy which is collected from the tracker solar panel in comparison with the total average energy collected from the static solar panel.

Calculating the area under the envelope of the generated energy curve for the solar tracking system gives us the total average energy ( $E_t$ ) = 25556.47 J/Day. As a result, the total average energy obtained from the solar tracking system that follow the sun by interval of 1 hour for 12 hours is equal to  $25556.47 - 10487.7 = 15068.77$  J/Day. On the other hand, the total average of the generated energy from the solar static system ( $E_s$ ) is equal to 11322.85 J/Day.

Using the equation (4.1), the efficiency of our system by using switching interval of 1 hour is 33.08%.

#### 4.2.2.9 Switching DC relay using an interval of 2 hours for 12 hours

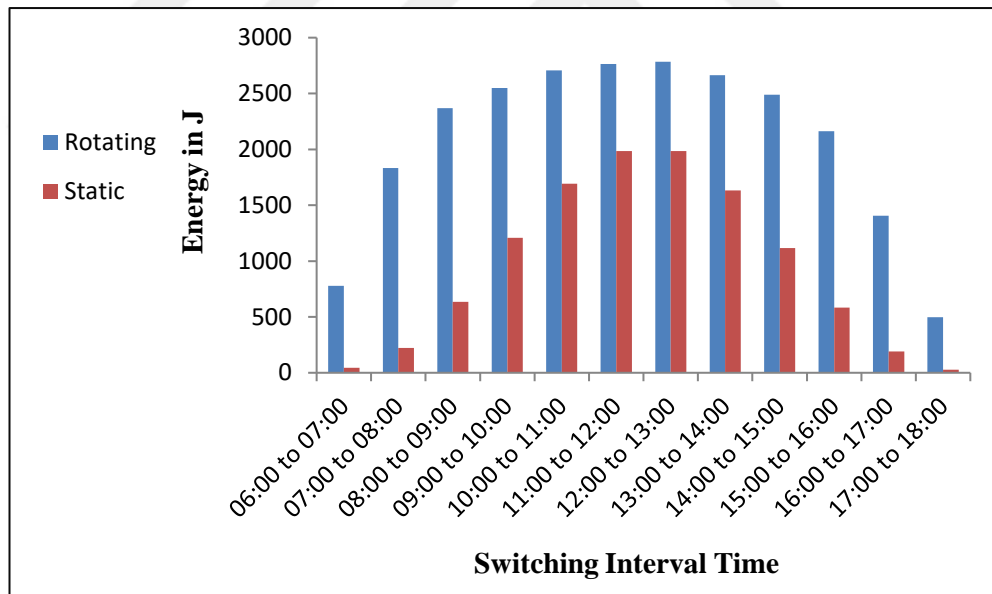


Figure 4.11: Rotating vs. static system for switching interval of 2 hrs.

The results illustrated in figure (4.11) shows the obtained energy from the static and the tracker panels. By using the tracking system, the maximum energy was 2784.24 J could be reached from 12:00 to 13:00. Contrastively, without using the solar tracking system (static system), the maximum energy reached from 12:00 to

13:00 is 1984.662 J. Also, the obtained energy of the tracker panel at any other time period is more than the obtained energy of the static panel at the same period.

Figure (4.11) also shows an increase in the total average energy which is collected from the tracker solar panel in comparison with the total average energy collected from the static solar panel.

Calculating the area under the envelope of the generated energy curve for the solar tracking system gives us the total average energy ( $E_t$ ) = 25003.98 J/Day. As a result, the total average energy obtained from the solar tracking system that follow the sun by interval of 2 hours for 12 hours is equal to  $25003.98 - 10475.28 = 14528.7$  J/Day. On the other hand, the total average of the generated energy from the solar static system ( $E_s$ ) is equal to 11322.85 J/Day.

Using the equation (4.1), the efficiency of our system by using switching interval of 2 hours is 28%.

#### 4.2.2.10 Switching DC relay using an interval of 3 hours for 12 hours

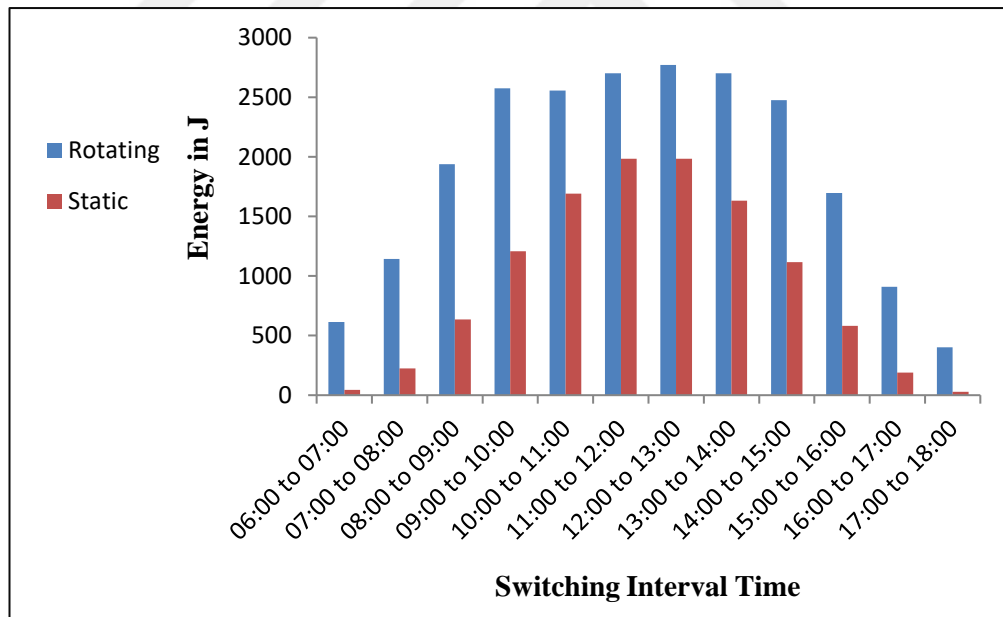


Figure 4.12: Rotating vs. static system for switching interval of 3 hrs.

The results illustrated in figure (4.12) shows the obtained energy from the static and the tracker panels. By using the tracking system, the maximum energy was 2771.64 J could be reached from 12:00 to 13:00. Contrastively, without using the solar tracking system (static system), the maximum energy reached from 12:00 to

13:00 is 1984.662 J. Also, the obtained energy of the tracker panel at any other time period is more than the obtained energy of the static panel at the same period.

Figure (4.12) also shows an increase in the total average energy which is collected from the tracker solar panel in comparison with the total average energy collected from the static solar panel.

Calculating the area under the envelope of the generated energy curve for the solar tracking system gives us the total average energy ( $E_t$ ) = 22482.36 J/Day. As a result, the total average energy obtained from the solar tracking system that follow the sun by interval of 3 hours for 12 hours is equal to  $22482.36 - 10471.14 = 12011.22$  J/Day. On the other hand, the total average of the generated energy from the solar static system ( $E_s$ ) is equal to 11322.85 J/Day.

Using the equation (4.1), the efficiency of our system by using switching interval of 3 hours is 6%.

#### 4.2.2.11 Switching DC relay using an interval of 4 hours for 12 hours

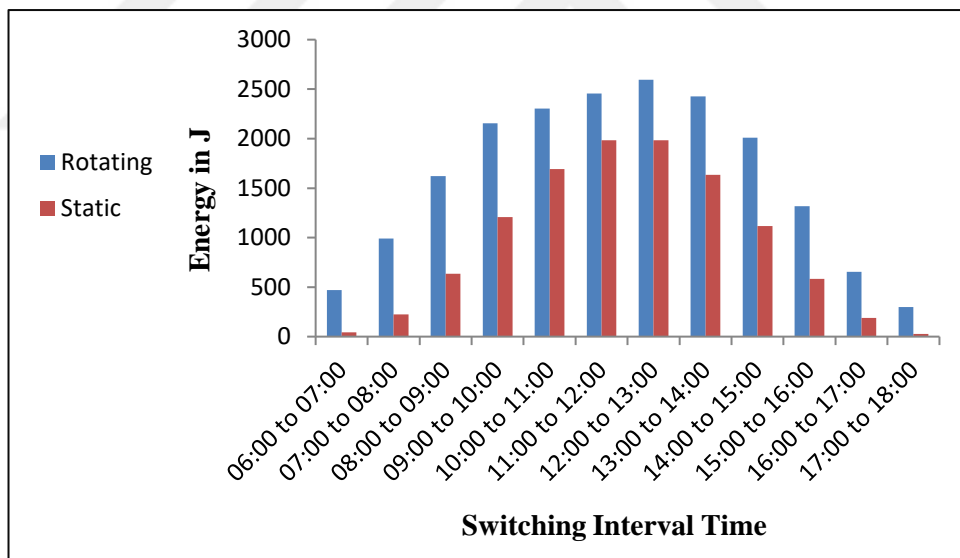


Figure 4.13: Rotating vs. static system for switching interval of 4 hrs.

The results illustrated in figure (4.13) shows the obtained energy from the static and the tracker panels. By using the tracking system, the maximum energy was 2593.56 J could be reached from 12:00 to 13:00. Contrastively, without using the solar tracking system (static system), the maximum energy reached from 12:00 to

13:00 is 1984.662 J. Also, the obtained energy of the tracker panel at any other time period is more than the obtained energy of the static panel at the same period.

Figure (4.13) also shows an increase in the total average energy which is collected from the tracker solar panel in comparison with the total average energy collected from the static solar panel.

Calculating the area under the envelope of the generated energy curve for the solar tracking system gives us the total average energy ( $E_t$ ) = 19293.9 J/Day. As a result, the total average energy obtained from the solar tracking system that follow the sun by interval of 4 hours for 12 hours is equal to  $19293.9 - 10469.07 = 8824.83$  J/Day. On the other hand, the total average of the generated energy from the solar static system ( $E_s$ ) is equal to 11322.85 J/Day.

Using the equation (4.1), the efficiency of our system by using switching interval of 4 hours is -22%.

#### 4.2.2.12 Switching DC relay using an interval of 6 hours for 12 hours

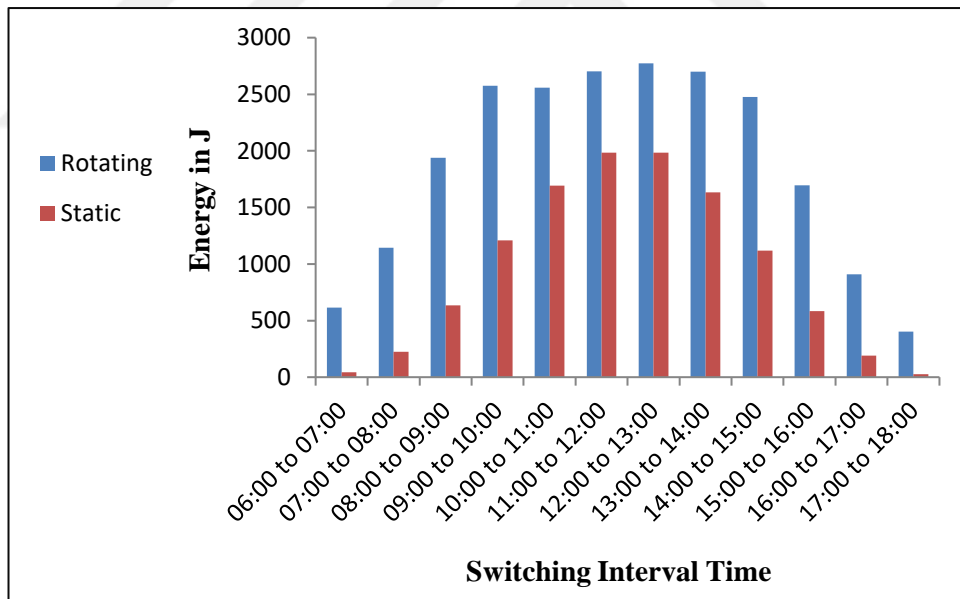


Figure 4.14: Rotating vs. static system for switching interval of 6 hrs.

The results illustrated in figure (4.14) shows the obtained energy from the static and the tracker panels. By using the tracking system, the maximum energy was 2771.64 J could be reached from 12:00 to 13:00. Contrastively, without using the solar tracking system (static system), the maximum energy reached from 12:00 to

13:00 is 1984.662 J. Also, the obtained energy of the tracker panel at any other time period is more than the obtained energy of the static panel at the same period.

Figure (4.14) also shows an increase in the total average energy which is collected from the tracker solar panel in comparison with the total average energy collected from the static solar panel.

Calculating the area under the envelope of the generated energy curve for the solar tracking system gives us the total average energy ( $E_t$ ) = 13857.3048 J/ Day. As a result, the total average energy obtained from the solar tracking system that follow the sun by interval of 6 hours for 12 hours is equal to  $13857.3048 - 10467 = 3390.3048$  J/Day. On the other hand, the total average of the generated energy from the solar static system ( $E_s$ ) is equal to 11322.85 J/Day.

Using the equation (4.1), the efficiency of our system by using switching interval of 6 hours is -70%.

### **4.3 Energy Consumption of The Prototype**

Here, we will consider that the continuous sun following system will switch the DC relay using an interval of 1 second. The Energy consumption of the control circuit is 10458.72 J and the energy needed to move the motors for 1 second is 89424 J as well as the motor needs energy to return to the start after the demise of the sun by 4.14 J. Therefore, the total energy consumption in the case of switching DC relay using an interval of 1 second for 12 hours is 99886.86 J and the table (4.2) explains the total energy consumption for the other different switching intervals.



**Table 4.2:** Energy consumption of the prototype for different intervals of time.

| Switching Interval Time | The Servo Motors Unit | The Control System Unit | Motor Return to Start | Total Energy Consumption |
|-------------------------|-----------------------|-------------------------|-----------------------|--------------------------|
| 5 mins                  | 298.08 J              | 10458.72 J              | 4.14 J                | 10760.94 J               |
| 10 mins                 | 149.04 J              | 10458.72 J              | 4.14 J                | 10611.9 J                |
| 20 mins                 | 74.52 J               | 10458.72 J              | 4.14 J                | 10537.38 J               |
| 30 mins                 | 49.68 J               | 10458.72 J              | 4.14 J                | 10512.54 J               |
| 40 mins                 | 37.26 J               | 10458.72 J              | 4.14 J                | 10500.12 J               |
| 50 mins                 | 29.808 J              | 10458.72 J              | 4.14 J                | 10492.67 J               |
| 55 mins                 | 27.098 J              | 10458.72 J              | 4.14 J                | 10489.96 J               |
| 1 hr                    | 24.84 J               | 10458.72 J              | 4.14 J                | 10487.7 J                |
| 2 hrs                   | 12.42 J               | 10458.72 J              | 4.14 J                | 10475.28 J               |
| 3 hrs                   | 8.28 J                | 10458.72 J              | 4.14 J                | 10471.14 J               |
| 4 hrs                   | 6.21 J                | 10458.72 J              | 4.14 J                | 10469.07 J               |
| 6 hrs                   | 4.14 J                | 10458.72 J              | 4.14 J                | 10467 J                  |

Note that, the total energy consumption of the proposed prototype increases when the switching interval time is also increased as shown in the Table (4.2).

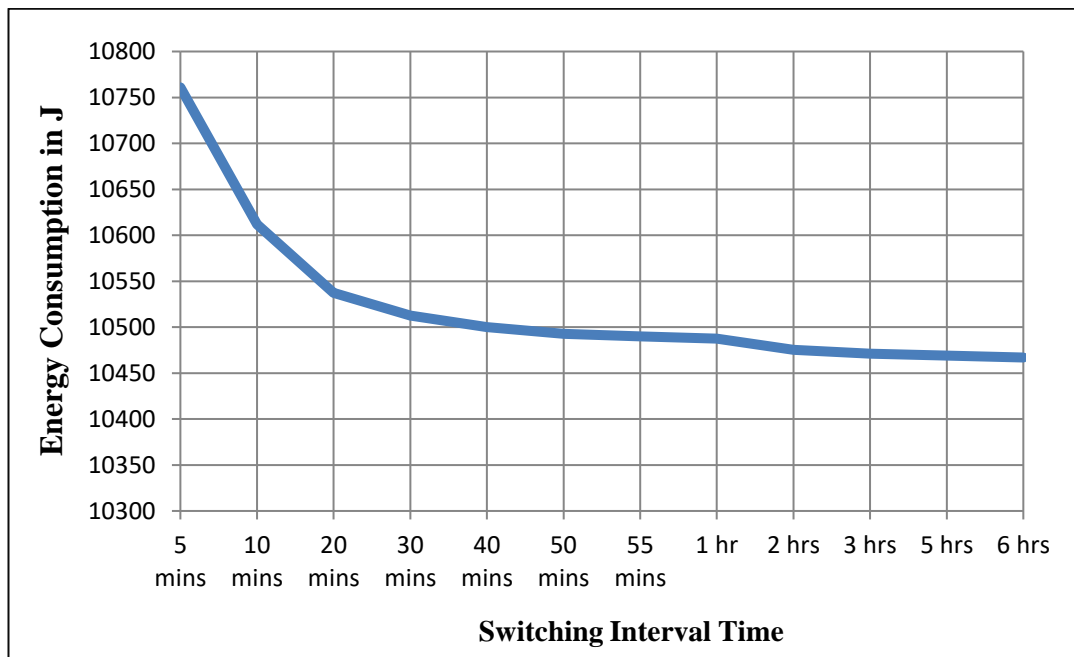


**Figure 4.15:** Energy consumption curve.

The highest total energy consumption appears in the case of switching the DC relay by using an interval of 5 minutes for 12 hours while the less total energy consumption appears in the case of switching the DC relay by using an interval of 6 hours as shown in figure (4.15).

#### 4.4 The Generated Energy Gain

We will consider that the difference between the total average of the generated energy and the total consumed energy as produced energy gain.

**Table 4.3:** Generated energy gain of the prototype for different intervals of time.

| Switching Interval Time | Generated Energy Gain in J |
|-------------------------|----------------------------|
| <b>5 mins</b>           | 15110.56                   |
| <b>10 mins</b>          | 15119.22                   |
| <b>20 mins</b>          | 15165.78                   |
| <b>30 mins</b>          | 15154.92                   |
| <b>40 mins</b>          | 15119.5                    |
| <b>50 mins</b>          | 15108.81                   |
| <b>55 mins</b>          | 15079.51                   |
| <b>1 hr</b>             | 15068.77                   |
| <b>2 hrs</b>            | 14528.7                    |
| <b>3 hrs</b>            | 12011.22                   |
| <b>4 hrs</b>            | 8824.83                    |
| <b>6 hrs</b>            | 3390.3048                  |

Note that, the generated energy gain of the proposed prototype increases when the switching interval time is also increased as shown in the Table (4.3).

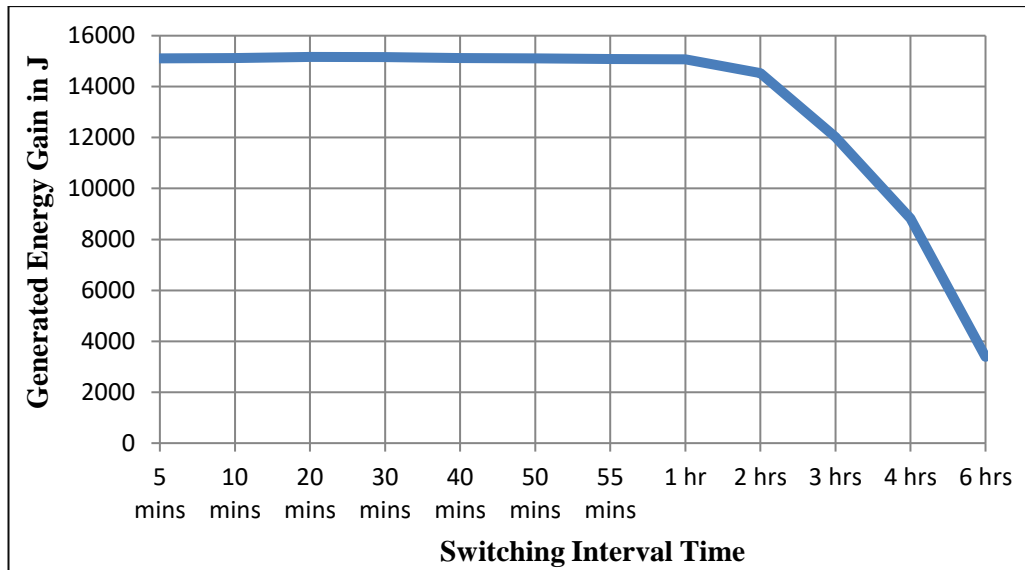


**Figure 4.16:** Generated energy gain curve.

The highest generated energy gain appears in the case of switching the DC relay by using an interval of 20 minutes for 12 hours while the less generated energy gain appears in the case of switching the DC relay by using an interval of 6 hours as shown in figure (4.16).

#### 4.5 Efficiency of The Proposed Prototype

It is the ratio of the difference between the total average of the generated energy of the tracking prototype and the total average of the generated energy of the static prototype to the total average generated energy of the static prototype.

**Table 4.4:** Efficiency percentage of the proposed prototype.

| Switching Interval Time | Efficiency (%) |
|-------------------------|----------------|
| <b>5 minutes</b>        | 33.45%         |
| <b>10 minutes</b>       | 33.5%          |
| <b>20 minutes</b>       | 34%            |
| <b>30 minutes</b>       | 33.8%          |
| <b>40 minutes</b>       | 33.53%         |
| <b>50 minutes</b>       | 33.44%         |
| <b>55 minutes</b>       | 33.18%         |
| <b>1 hour</b>           | 33.08%         |

**Table 4.4 (Continued):** Efficiency percentage of the proposed prototype.

| Switching Interval Time | Efficiency (%) |
|-------------------------|----------------|
| <b>2 hours</b>          | 28%            |
| <b>3 hours</b>          | 6%             |
| <b>4 hours</b>          | -22%           |
| <b>6 hours</b>          | -70%           |

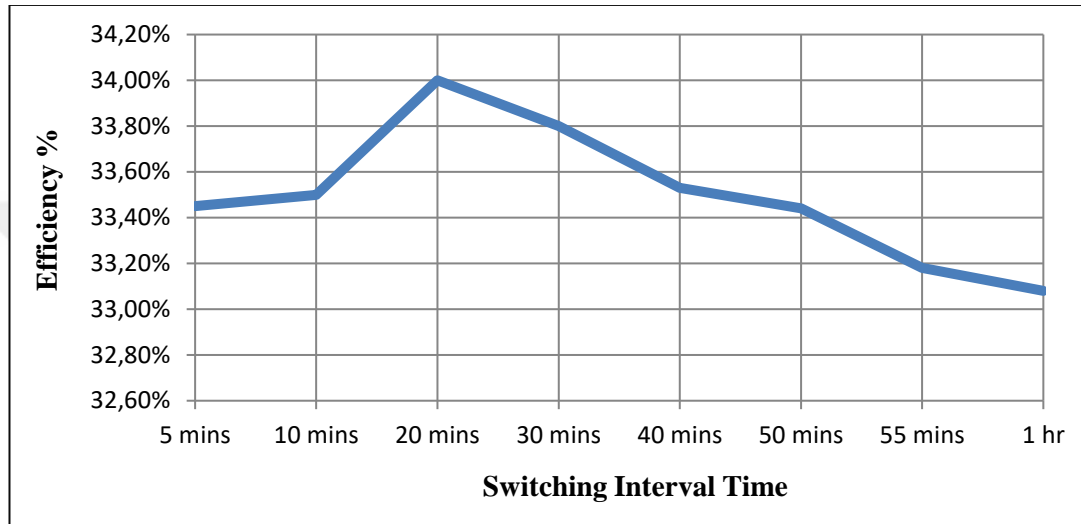


**Figure 4.17:** Efficiency curve of the proposed prototype.

The highest efficiency appears in the case of switching the DC relay by using an interval of 20 minutes for 12 hours by 34% as shown in figure (4.17).

## **CHAPTER FIVE**

### **CONCLUSIONS AND FUTURE WORKS**

#### **5.1 Conclusions**

In this work, we designed and implemented a dual axis solar tracker prototype to track the movement of the sun as the sun rises from the east and sets into the west during the day. Our prototype has been designed by using AutoCAD 2017. The mechanical parts have been cut by using a Computer Numerical Control (CNC). The control circuit was achieved by using the AVR microcontroller and Proteus simulation programs and it has been practically tested.

We also proposed to use PVC foam material in order to reduce the weight of the prototype and decrease the energy consumption. Likewise, PVC foam material can withstand the high temperatures of Iraq weather that can arrive to 56°C.

For decreasing the energy consumption and increasing the efficiency of the prototype, we propose the discretizing for the tracking operation of sun position by using a switching DC relay. The optimal switching interval was 20 minutes that increased the efficiency of our prototype to 34%. This optimal tracking period saved 89.45% of the requested energy for the control circuit in comparison with the continuous tracking system.

Our proposed dual axis solar tracking prototype is more advantageous for capturing the maximum sunlight with increasing the average power by 34% in comparison with the static solar system which using the optimal switching interval.

#### **5.2 Future Works**

According to the results and the experiments in this thesis, many suggestions can be proposed to develop the tracking design for the future as follows:

1. Studying the optimal switching interval for larger solar panels.
2. Replacing the control circuit of our prototype system with another control circuit can consume less energy such as STM32 Nucleo-64 development board with STM32F401RE MCU.

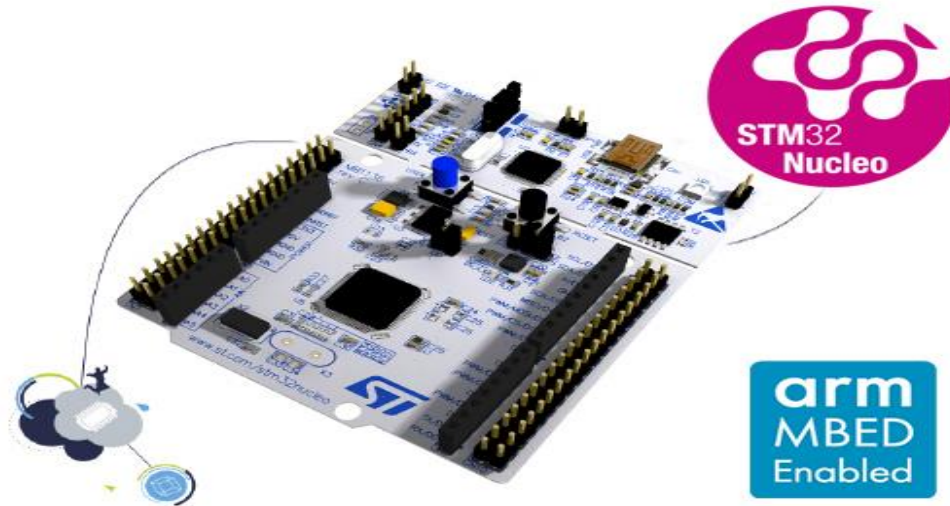


**Figure 5.1:** STM32 Nucleo-64 development board with STM32F401RE MCU.

## REFERENCES

- [1] Stamatescu, I., Stamatescu, G., Arghira, N., Fagarasan, I., & Iliescu, S. S. (2014). Fuzzy decision support system for solar tracking optimization. *2014 International Conference on Development and Application Systems (DAS)*, 16-20.
- [2] Ahmad, S., Shafie, S., & Kadir, M. Z. (2012). A high power generation, low power consumption solar tracker. *2012 IEEE International Conference on Power and Energy (PECon)*, 366-371.
- [3] Alexandru, C. (2009). The design and optimization of a photovoltaic tracking mechanism. *2009 International Conference on Power Engineering, Energy and Electrical Drives*, 436-441.
- [4] Usta, M. A., Akyazı, Ö, & Altaş, İ. H. (2011). *Design and Performance of Solar Tracking System with Fuzzy Logic Controller* (pp. 381-385). Elazığ, Turkey: 6th International Advanced Technologies Symposium (IATS'11).
- [5] Pagliaro, M., Ciriminna, R., & Palmisano, G. (2009). *Flexible solar cells*. Weinheim: Wiley-VCH.
- [6] *Photovoltaics technical information guide: a product of the Solar Technical Information Program*. (1985). Golden, CO: Technical Information Branch, Solar Energy Research Institute.
- [7] Tudorache, T., & Kreindler, L. (2010). Design of a Solar Tracker System for PV Power Plants. *Acta Polytechnica Hungarica*, 7, 23-39.
- [8] Ozcelik, S., Prakash, H., & Chaloo, R. (2011). Two-Axis Solar Tracker Analysis and Control for Maximum Power Generation. *Procedia Computer Science*, 6, 457-462.
- [9] Dolara, A., Grimaccia, F., Leva, S., Mussetta, M., Faranda, R., & Gualdoni, M. (2012). Performance Analysis of a Single-Axis Tracking PV System. *IEEE Journal of Photovoltaics*, 2(4), 524-531.

- [10] Waheed, A. R. (2013). *Implementation of solar energy tracking system using microcontroller* (Unpublished master's thesis). Electrical Engineering, University of Technology-Iraq.
- [11] Bin Azman, A. A. (2014). *A solar tracking system with multiple input parameters for efficiency optimization* (master's thesis). Faculty of Electrical Engineering, Universiti Teknologi Malaysia.
- [12] Asyraf, M. A. (2015). *Design of low power automatic sun tracking system using arduino uno* (master's thesis). Faculty of Electrical Engineering, Universiti Teknologi Malaysia.
- [13] K, V. (2016). Designing a Dual Axis Solar Tracking System for Maximum Power. *Journal of Electrical & Electronic Systems*, 5(3), 1.
- [14] Banerjee, R. (2015). Solar Tracking System. *International Journal of Scientific and Research Publications*, 5(3), 1-6.
- [15] Bezawada, H. V., Sekha, A. S., & Reddy, K. S. (2014). Design and Analysis of Dual Axes Tracking System for Solar Photovoltaic Modules. *International Journal of Engineering Development and Research*, 2(3), 3181-3189.
- [16] Puranik, H. N., Quamar, N., Kumar, N., & Bhambore, I. (2016). Design and Implementation of Sun Tracker Solar Panel with Smart Monitoring System. *International Journal of Advanced Research in Electrical, Electronics and Instrumentation Engineering*, 5(4), 2904-2910.
- [17] Bazyari, S., Keypour, R., Farhangi, S., Ghaedi, A., & Bazyari, K. (2014). A Study on the Effects of Solar Tracking Systems on the Performance of Photovoltaic Power Plants. *Journal of Power and Energy Engineering*, 02(04), 718-728.
- [18] Bonkougou, D., Koalaga, Z., & Njomo, D. (2013). Modelling and Simulation of photovoltaic module considering single-diode equivalent circuit model in MATLAB. *International Journal of Emerging Technology and Advanced Engineering*, 3(3), 493-502.
- [19] Bagher, A. M., Abadi, M. M., Vahid, & Mohsen, M. (2015). Types of Solar Cells and Application. *American Journal of Optics and Photonics*, 3(5), 94-113.
- [20] Douglass, S. E., Junkans, D. A., & Kurtz, L. S. (2005). *Identifying the Opportunities in Alternative Energy* (pp. 9-10, Rep.). Private Client Services.



## **CURRICULUM VITAE**

### **PERSONAL INFORMATION**

Surname, Name : Omar Talib Taha KHAZRAJI

Nationality : IRAQI

Date and Place of Birth : 10.04.1992 - IRAQ. Baghdad

Phone : +90 (534) 970 83 68

Email : omartalib1212@gmail.com

### **EDUCATION**

| Degree      | Institution                                     | Year of Graduation |
|-------------|---|--------------------|
| MS          | University of Turkish Aeronautical Association  | 2017               |
| BS          | College of Electrical and Electronic Technology | 2014               |
| High School | Al-Khazlia School                               | 2010               |

### **FOREIGN LANGUAGES**

English, Turkish